

**FOCUSED FEASIBILITY STUDY REPORT
FOR
40TH AVENUE PROJECT AREA
IN THE ST. LOUIS RIVER AREA OF CONCERN**

August 28, 2015

APPENDIX N. USACE SEDIMENT TRANSPORT MODELING



US Army Corps
of Engineers®
Engineer Research and
Development Center

Sediment Transport Modeling for the St. Louis River Estuary 40th Ave Shoals and Islands Designs

April 2015

Earl Hayter, Ray Chapman, Phu Luong, Greg Mausolf, and Lihwa Lin

*Environmental and Coastal and Hydraulics Laboratories
U.S. Army Engineer Research and Development Center
3909 Halls Ferry Road
Vicksburg, MS 39180*

Letter Report

Sediment Transport Modeling for the St. Louis River Estuary 40th Ave Shoals and Islands Designs

Earl Hayter

*Environmental Laboratory
U.S. Army Engineer Research and Development Center
3909 Halls Ferry Road
Vicksburg, MS 39180-6199*

Ray Chapman, Phu Luong , and Lihwa Lin

*Coastal and Hydraulics Laboratory
U.S. Army Engineer Research and Development Center
3909 Halls Ferry Road
Vicksburg, MS 39180-6199*

Greg Mausolf

*U.S. Army Corps of Engineers, Detroit District
477 Michigan Avenue
Detroit, MI 4822*

Letter Report

Approved for public release; distribution is unlimited.

**Prepared for U.S. Army Engineer District, Detroit
Detroit, MI 48226**

Abstract

The U.S. Army Corps of Engineers (USACE) Detroit District (LRE) Hydraulics and Hydrology Office (H&H) is working with the US Army Engineer Research and Development Center (ERDC) Environmental (EL) and Coastal and Hydraulics Laboratories (CHL) to perform a numerical modeling study to determine if dredged material used to create both shoals and islands would stay within the area of placement at the 40th Avenue Area of Concern (AOC), which is located along the western shore of Duluth harbor. The numerical modeling study consisted of applying the Geophysical Scale Transport Modeling System (GSMB) to simulate the hydrodynamics, sediment transport and waves in the St Louis River – Duluth Harbor estuarine system during the design event chosen by LRE. The modeling results were analyzed to determine the location and quantity of net erosion that occurs in proximity to the designed islands and shoals features over the simulated event. The sediment transport model was run assuming a grain size distribution of the typical placed dredged material of 50% coarse (*i.e.*, sand size sediment) and 50% fines (*i.e.*, silt size sediment).

The main conclusion from the modeling for both designs is that minimal net erosion occurred over the simulated four-month period. Some areas of net erosion were predicted to occur on top of the shoals and around some of the shorelines of the islands. The following two factors contribute jointly to the overall minimal net erosion:

- The short period wind waves that are generated inside the harbor do not affect the calculated bed shear stresses unless the water depths are fairly shallow. This reduces the areas where erosion occurs.
- The 40th Ave embayment is off the main channel/river, so the flows in this area, that are the result of wind generated circulation as well as circulation resulting from flow separation off the point of land immediately to the south of this embayment, are low except during large events. These low flows also contribute to the relatively small amount of net erosion that is simulated to occur over the modeled four-month period.

Contents

1	Introduction	1
	Objectives	1
	Study Tasks	1
2	Hydrodynamic Modeling	4
	GSMB Modeling System	4
	Selection of Simulation Event	5
	ADCIRC Simulations	7
	Multi-Block Hydrodynamic Model Simulations	8
3	Wave Modeling	17
	Purpose	17
	Wave Model	17
	Model Setup	18
	Model Simulations	20
4	Sediment Transport Modeling	22
	Setup of SEDZLJ	22
	Modeling Results	24
5	Conclusions	28
	References	29
	Appendix A: Description of the CMS-Wave model	33
	Appendix B: Description of the SEDZLJ sediment bed model	36

Figures and Tables

Figures

Figure 1-1. Duluth Harbor – St. Louis River Area.....	2
Figure 2-1. Geophysical Scale Transport (GSMB) Modeling System	4
Figure 2-2. St. Louis River Flow Record from March 1 (Day 60) to August 1 (Day 213), 2008	5
Figure 2-3. Wind Rose for Simulation Period (27-March-2008 through 26-July-2008) generated from Duluth NOAA station meteorological data	6
Figure 2-4. Water levels for 2008 from NOAA Station at Duluth, MN.....	7
Figure 2-5. Lake Superior IGLD85 Bathymetry	8
Figure 2-6. Lake Superior ADCIRC Grid	8
Figure 2-7. Model Domain for the DH-SLR Ch3D-SEDZLJ model	10
Figure 2-8. Initial Single Block Grid.....	10
Figure 2-9. 18 Block Grid of the DH-SLR Model Domain.....	11
Figure 2-10. Block 5 with Shoals Design	12
Figure 2-11. Block 5 with Islands Design.....	13
Figure 2-12. Nemadji River Flow Record	14
Figure 2-13a Wind Speed Record Measured at the Duluth NOAA Station.....	15
Figure 2-13b Wind Direction Record Measured at the Duluth NOAA Station.....	15
Figure 2-14 WLSSD Daily Average Discharges.....	16
Figure 3-1. CMS-Wave model domain and depth Contours.....	18
Figure 3-2. NOAA Station 9099064 wind data for March to July 2008.....	19
Figure 3-3. NOAA Station 9099064 water level data for March to July 2008.....	19
Figure 3-4. Calculated wave field, 0200 GMT 11 April 2008	20
Figure 3-5. Calculated wave field, 2100 GMT 06 June 2008	21
Figure 4-1. Color contoured plot of the net negative change in bed elevation in Block 5 for the shoals design	25
Figure 4-2. Zoomed in color contoured plot of the net negative change in bed elevation in Block 5 and the shapes of the shoals	26
Figure 4-3. Color contoured plot of the net negative change in bed elevation in Block 5 for the islands design	27
Figure A-1. The CMS framework and its components	34
Figure B-1. Sediment transport processes simulated in SEDZLJ	38
Figure B-2. Multi-bed layer model used in SEDZLJ	40
Figure B-3. Schematic of Active Layer used in SEDZLJ.....	40

Tables

Table 4-1. Settling Velocities of the Eight Modeled Sediment Sizes	23
Table 4-2. Percentages of Sediment Size Classes for Sediment Types.....	24

1 Introduction

The U.S. Army Corps of Engineers (USACE) Detroit District (LRE) Hydraulics and Hydrology Office (H&H) had the US Army Engineer Research and Development Center (ERDC) Environmental (EL) and Coastal and Hydraulics Laboratories (CHL) perform a numerical modeling study to investigate the placement of dredged material to create both shoals and islands in an Area of Concern (AOC) in the St. Louis River – Duluth Harbor system (see Figure 1-1).

Objectives

The objectives of ERDC's modeling study as requested by LRE were the following:

1. Develop a numerical hydrodynamic and sediment transport modeling system that could be used to evaluate the stability of dredged material used to create shoals and islands in the 40th Avenue Area of Concern (AOC) during a simulated high-energy wind and flow event.
2. Perform the sediment transport modeling study using the following two designs for the 40th Avenue AOC: 1) placed dredged material used to create shoals; and 2) placed dredged material used to create islands.
3. Analyze the results from the modeling study of both AOC designs to determine the magnitude and locations of net erosion in proximity to the design shoal and island features.

Study Tasks

The following specific tasks were performed to accomplish the stated objectives.

Task 1. Develop Modeling System for Duluth Harbor – St. Louis River

ERDC's Geophysical Scale Transport Modeling System (GSMB) was applied to this estuarine system. GSMB is described in Section 2. It contains the mixed sediment transport model (that is dynamically linked to the hydrodynamic model) that was used to simulate the transport of both placed dredged material and native sediments.

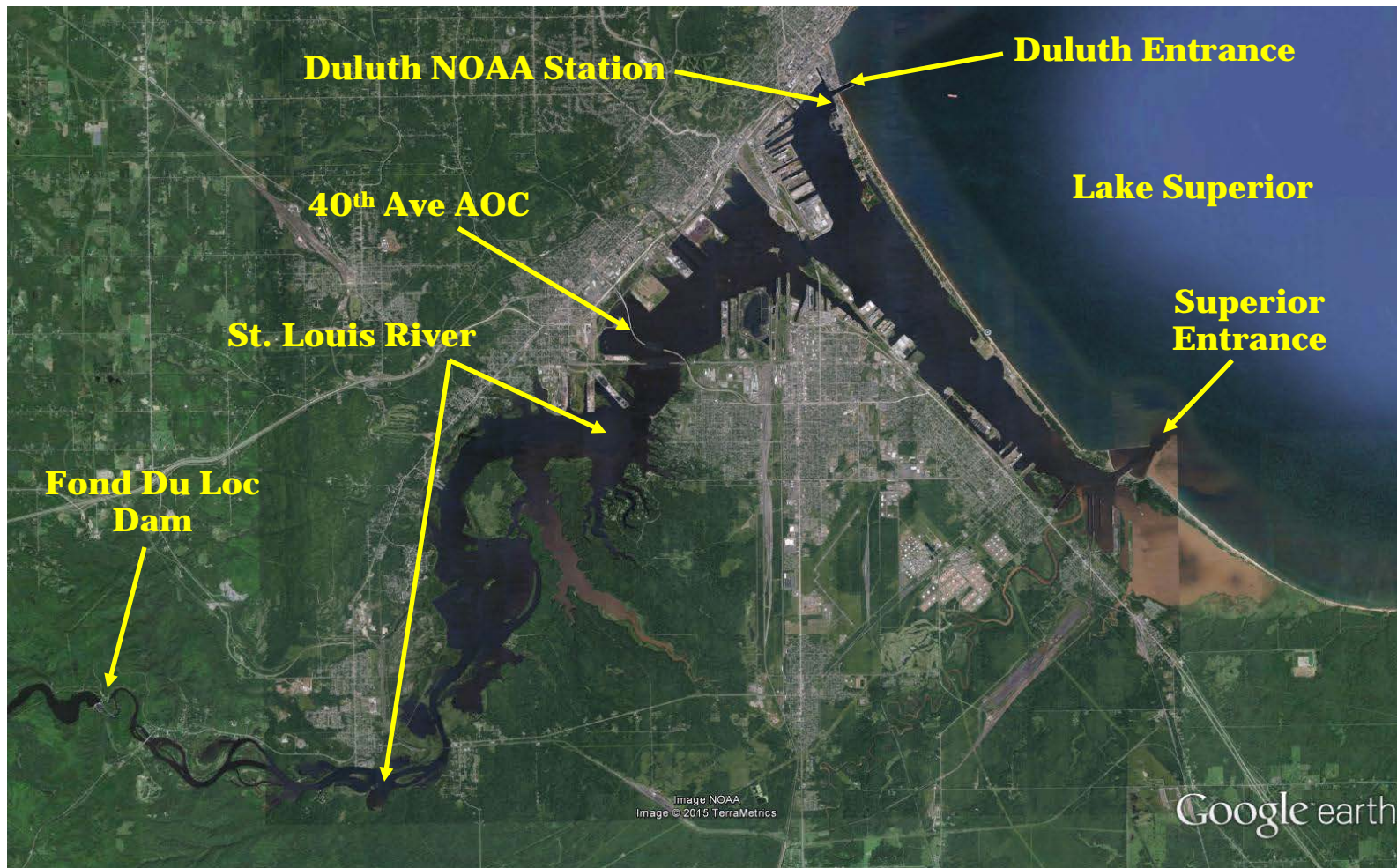


Figure 1-1 Duluth Harbor – St. Louis River Area

Task 2. Hydrodynamic Modeling

The hydrodynamic module of GSMB, described in Section 2, was applied to simulate the high-energy event selected by LRE to insure a stable hydrodynamic environment for the sediment transport modeling.

Task 3. Wave Modeling

The CMS-Wave model, which is a spectral wave transformation model capable of simulating the formation, diffraction, refraction, reflection, and breaking of wind-generated surface waves, was used to model the selected event. This modeling is described in Section 3. Time series of wave properties (wave heights, periods and directions) were used in the mixed sediment transport model in GSMB to calculate the spatially and temporally varying current- and wave-induced bed shear stresses.

Task 4. Sediment Transport Modeling

The mixed sediment transport module of GSMB was setup using data analyzed by ERDC from dredged material placed at the 21st Ave W AOC site. The sediment transport modeling performed for the two 40th Ave designs is described in Section 4.

Task 5. Analysis of Modeling Results

The results of the sediment transport modeling were analyzed to determine the areas in the 40th Ave AOC where net erosion over the chosen event was simulated to occur. The results from this analysis are described in Section 5.

2 Hydrodynamic Modeling

GSMB Modeling System

ERDC-EL and ERDC-CHL have completed a number of large scale hydrodynamic, sediment and water quality transport modeling studies. These studies have been successfully executed utilizing the Geophysical Scale Transport Modeling System (GSMB). The model framework of GSMB is shown in Figure 2-1, where it is seen that USACE accepted wave, hydrodynamic, sediment and water quality transport models are both directly and indirectly linked.

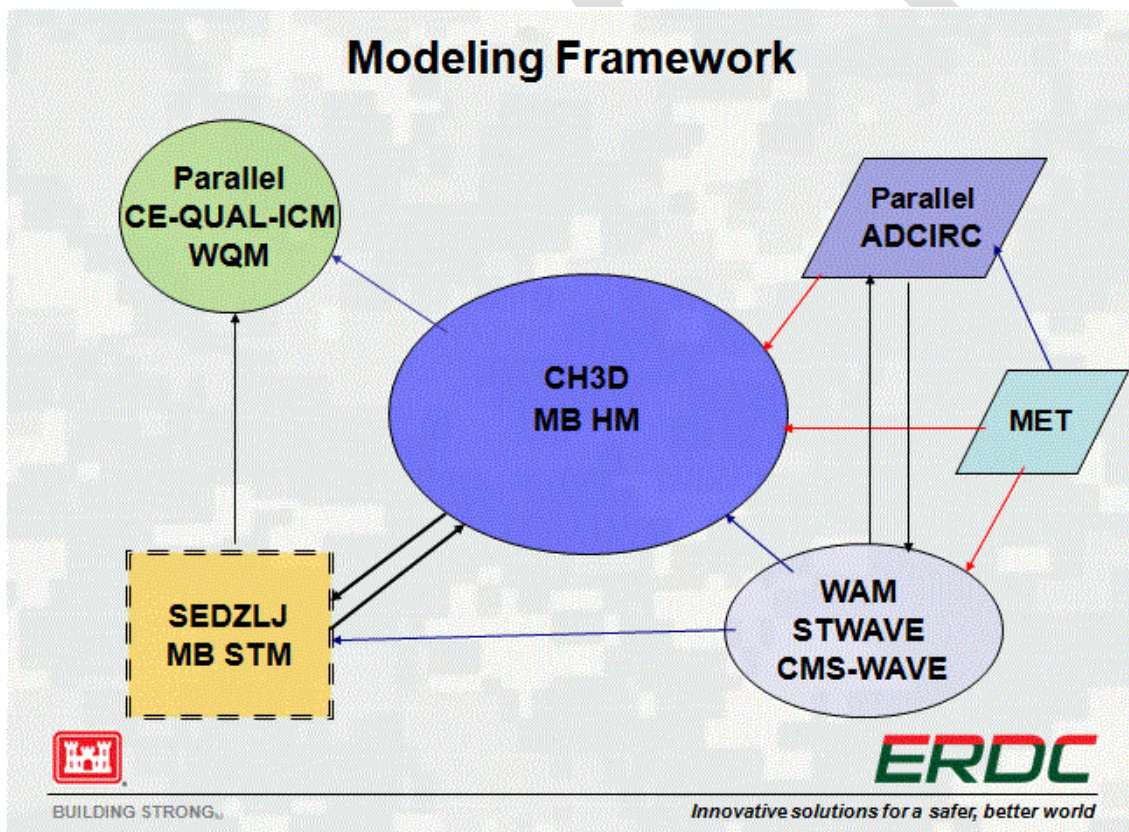


Figure 2-1 Geophysical Scale Transport (GSMB) Modeling System

The components of GSMB are the 2D deep water wave model WAM (Komen *et al.* 1994, and Jensen *et al.* 2012); shallow water wave models STWAVE (Smith *et al.* 1999) and CMS-WAVE (Lin *et al.* 2008); the large scale unstructured 2D ADCIRC hydrodynamic model (<http://www.adcirc.org>); and the regional scale models CH3D-

MB (Luong and Chapman 2009), which is the multi-block (MB) version of CH3D-WES (Chapman *et al.* 1996; Chapman *et al.* 2009), MB CH3D-SEDZLJ sediment transport model (Hayter *et al.* 2012), and CE-QUAL-ICM water quality model (Bunch *et al.* 2003, and Cerco and Cole 1994). For this study, a subset of GSMB components was applied where the meteorologically forced WAM provides the deep water spectral wave data (<http://wis.usace.army.mil/hindcasts.shtml>) to CMS-WAVE, which in turn provides wave heights, periods and directions forcing to the GSMB sediment transport module. In addition, open water surface elevation forcing is provided by ADCIRC. The latter is described later in this chapter.

Selection of High Energy Event to Simulate

After examining water level and wind records for multiple meteorological events over a 20 year period, LRE selected the four month period of March 27 – July 26 (121 days), 2008 to simulate using the GSMB modeling system. This period was chosen because it included a couple of large storms and two high flow events in the St. Louis River. Forcing conditions during this four month period are described next.

- The flow record at the Fond Du Lac dam (see Figure 1-1), which is the upstream boundary of the GSMB model domain, is shown in Figure 2-2. The x-axis is plotted in days from Day 60 to Day 213. The simulated March 27 – July 26 period is from Day 87 to Day 213. As seen below, this period includes the snow melt induced high flow event that peaks near May 1 (Day 121). The

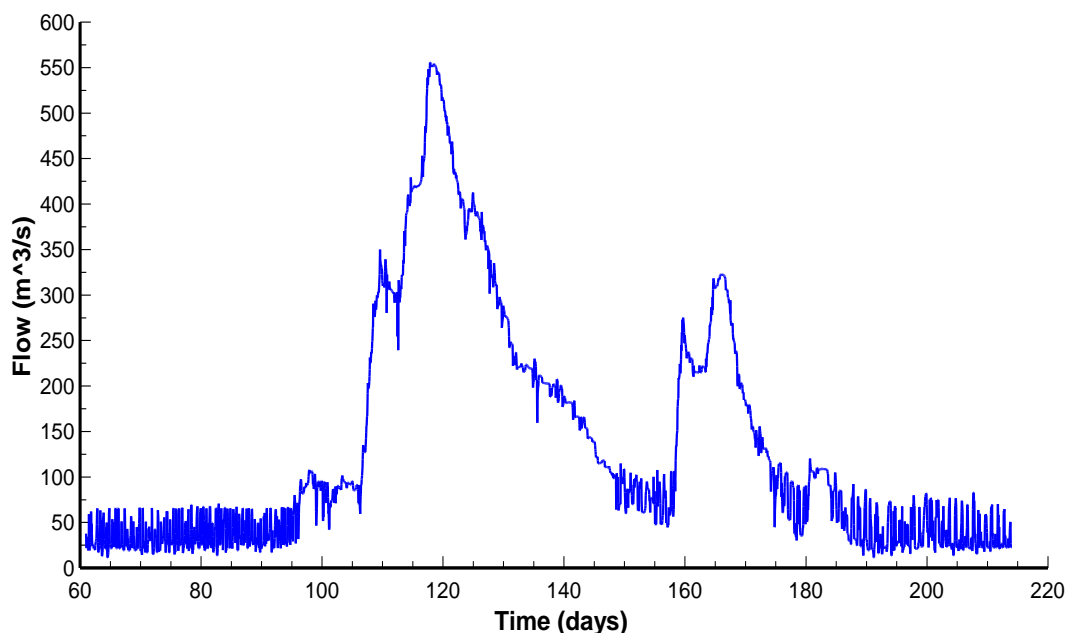


Figure 2-2 St. Louis River Flow Record from March 1 (Day 60) to August 1 (Day 213), 2008.

flow for the high flow event of 575 m³/s (cms) (20,300 cfs) is representative of a 30% annual exceedance probability, or an approximate three-year flow event. It also includes a relatively high flow event that spans Days 160 to 175 (June 8 – 23).

- The wind rose for the simulated March 27 – July 26 period (Day 87 to Day 213) is shown in Figure 2-3. This shows that the highest wind speeds during this four month period were from the northeast, which is the direction for which the fetch is by far the greatest at the 40th Ave AOC. This will produce the highest waves in the 40th Ave embayment.

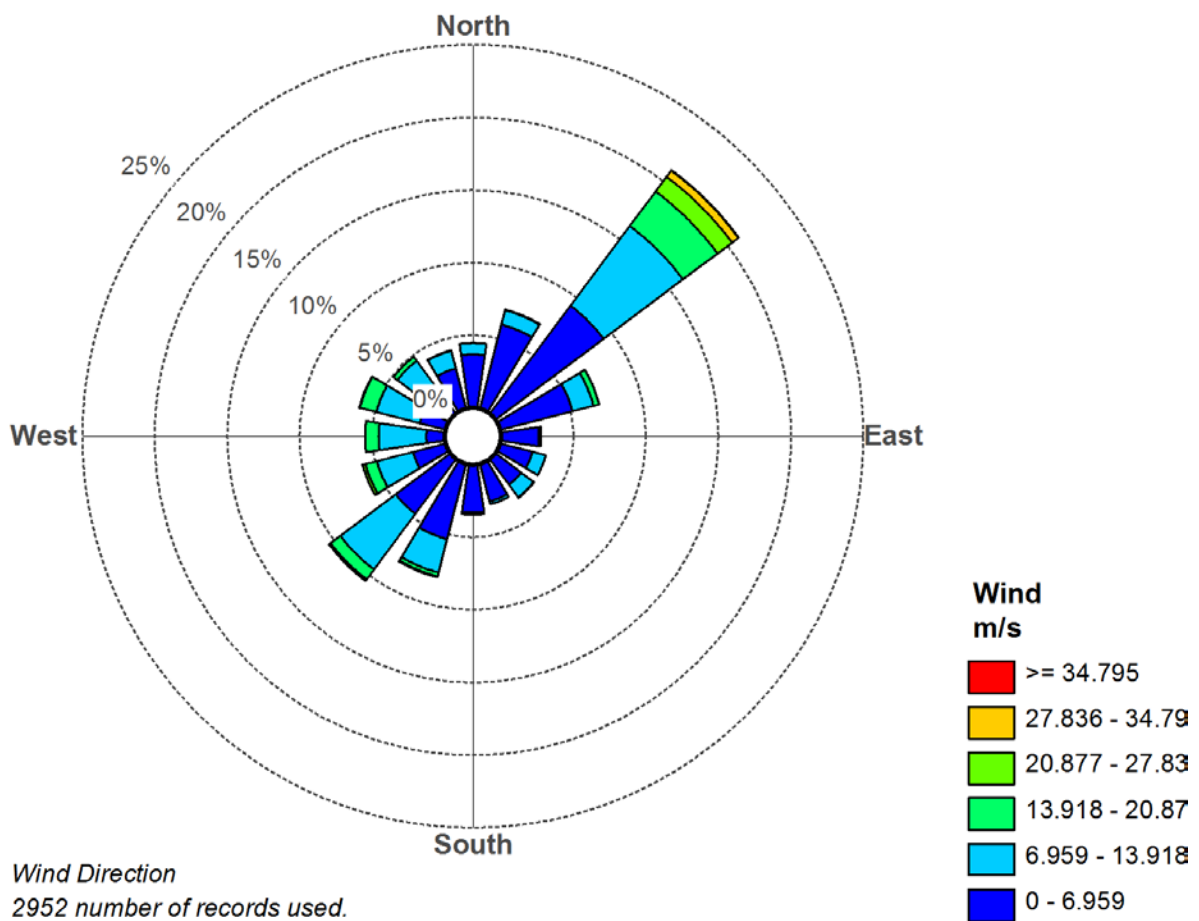


Figure 2-3 Wind Rose for Simulation Period (27-March-2008 through 26-July-2008) generated from Duluth NOAA station meteorological data

- Figure 2-4 shows the daily water levels measured for 2008 at the NOAA 9099064 station just inside the Duluth entrance (see Figure 1-1) to Duluth

Harbor. As seen, there is a 1.5 ft (0.46 m) increase in the water level over the selected four month period.

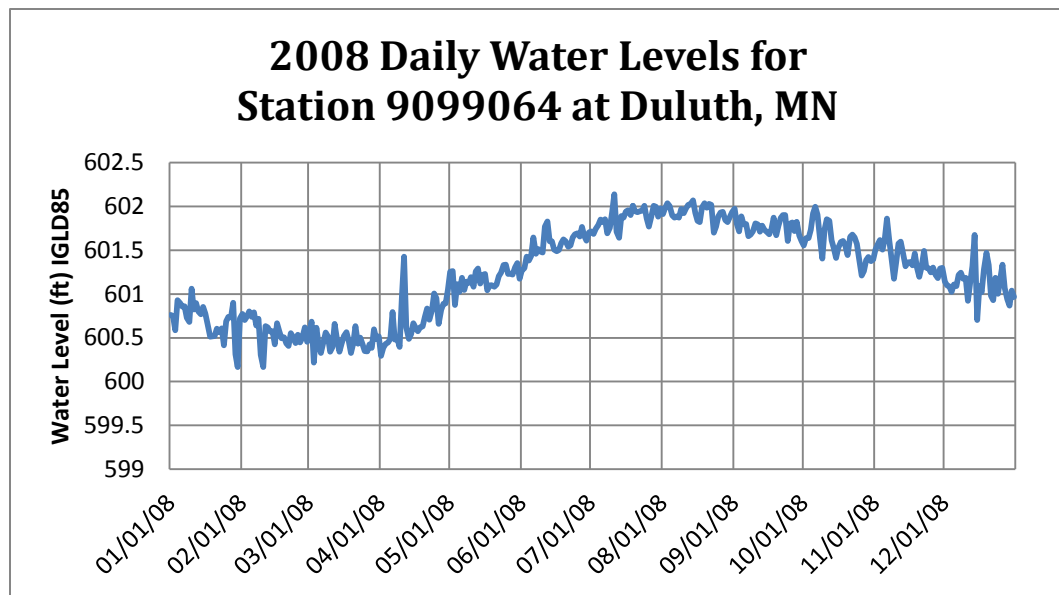


Figure 2-4 Water levels for 2008 from NOAA Station at Duluth, MN

ADCIRC Simulations

The existing ADCIRC storm surge model bathymetry and grid, which were provided by the FEMA Modeling Contractor STARR (2012), are shown in Figures 2-2 and 2-3, respectively. The Lake Superior ADCIRC model was driven by wind and pressure fields generated by Oceanweather Inc. (under contract to LRE for a 2012 FEMA project) using the NCEP Climate Forecast System Reanalysis (CFSR) archive. The archive is based on a reanalysis of all meteorological products generated by NOAA's National Center for Environmental Predictions (<http://rda.ucar.edu/pub/cfsr.html>). This 33-year archive (1979 to 2011) provides wind and pressure on a Gaussian grid with resolution of approximately 38 km, and barometric pressure fields on a 0.5 degree global geographical resolution at one-hour intervals. The Lake Superior wind and pressure fields were downloaded, interpolated from the Gaussian grid to a spherical grid with a resolution of 0.02 degree in both longitude and latitude and reformatted by Oceanweather Inc. Using this model, extensive calibration and validation storm event simulations were performed and analyzed by STARR (2012).

The calibrated and validated Lake Superior ADCIRC model was used to simulate the four month period 27 March – 26 July 2008. The simulated water surface elevations along the open water boundary in the model domain for the GSMB hydrodynamic and sediment transport modules were extracted from the ADCIRC output files.

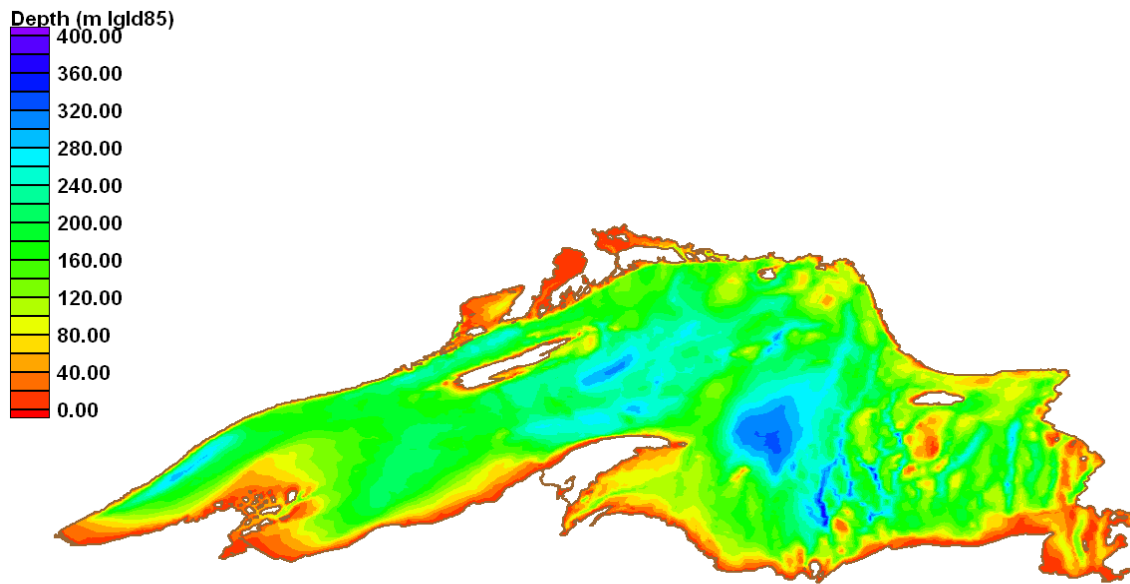


Figure 2-5 Lake Superior IGLD85 Bathymetry

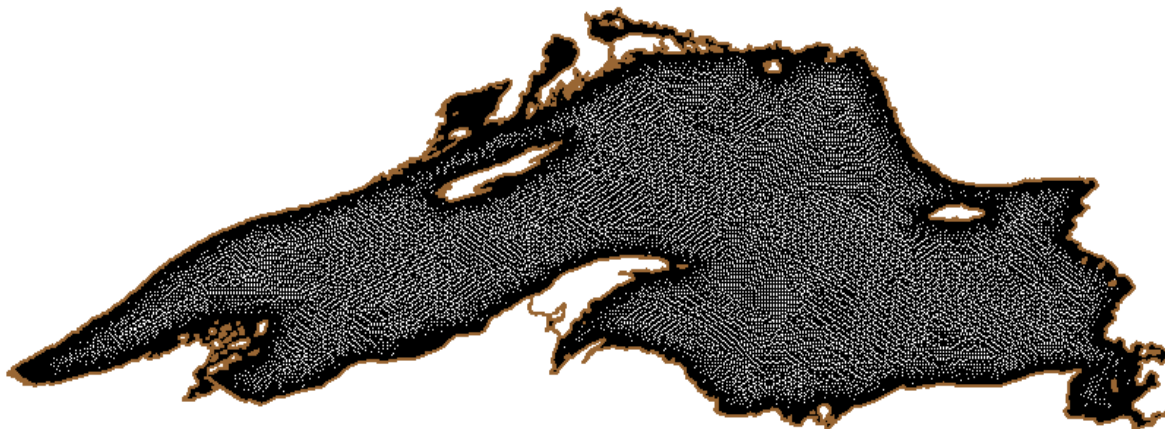


Figure 2-6 Lake Superior ADCIRC Grid

Multi-Block Hydrodynamic Model Simulations

Hydrodynamic modeling of the Duluth Harbor – St. Louis River estuary (DH-SLR) was performed with the GSMB hydrodynamic module. Previous single-block applications of combined hydrodynamic and sediment transport models, *e.g.*, the EFDC model developed for DH-SLR and used to simulate sediment transport of dredged material placed at the 21st Ave West AOC in 2013 (Mausolf 2014) required long computer processing time as well as large memory storage requirements. This is because in structured grids with complicated geometries, the number of active cells

(water) is often much smaller than the number of inactive cells (land). Both of these issues are overcome by implementation of single-block grid decomposition and Message Passing Interface (MPI) subroutines, which provide the multi-block grid capability (Snir *et al.* 1998). The MB grid approach runs each grid in parallel computations, where each grid block is assigned to a separate CPU or processor. Message passing allows the exchange of computational field information, such as the water surface elevation, velocity component and constituent arrays, between adjacent grid blocks. The advantages of the MB grid parallel approach include 1) the flexibility of site specific horizontal and vertical grid resolution assigned to each grid block, 2) block specific application of the sediment transport, wave radiation stress gradient forcing and computational cell wetting/drying model options and 3) reduced memory and computational time requirements allowing larger computational domains and longer simulation time periods. Recent applications of the GSMB modeling system have included Mississippi Sound, which is a micro-tidal environment (Chapman and Luong 2009), and Cook Inlet, AK, which is a hypertidal estuary (Hayter *et al.* 2013).

The model domain for the GSMB model developed for the present study is shown in Figure 2-7. This domain was chosen to insure that the two main boundaries (upstream boundary of the SLR at the Fond Du Lac dam and the Lake Superior open water boundary) are sufficiently remote to the 40th Ave AOC site to not directly impact the simulated flows and sediment transport in proximity to the AOC site. The bathymetry used in the MB grid was provided by LRE. Initially a single-block grid of the entire model domain was developed (see Figure 2-8). This was then divided into 18 blocks (see Figure 2-9). The initial 18-block grid model is henceforth referred to as the DH-SLR base model. To represent the designed shoals and islands and the modified bathymetry in the 40th Ave AOC, Blocks 5 and 6 were modified. The two modified versions of Block 5 (that includes the 40th Ave AOC) are shown in Figures 2-10 and 2-11.

The water surface elevation forcings along the open water boundary in Lake Superior (see Figure 2-7) were developed using the results from the ADCIRC simulation discussed in the previous section. To account for the seasonal lake level variation in the boundary forcing, *i.e.*, the 1.5 ft (0.46 m) increase in the lake level over the four-month simulation period, the observed water level data (shown in Figure 2-4) was time averaged to develop a set of linear segments that were added to the boundary input. This enabled the 1.5 ft rise in the water level in Lake Superior to be represented in the CH3D-SEDZLJ model simulations.

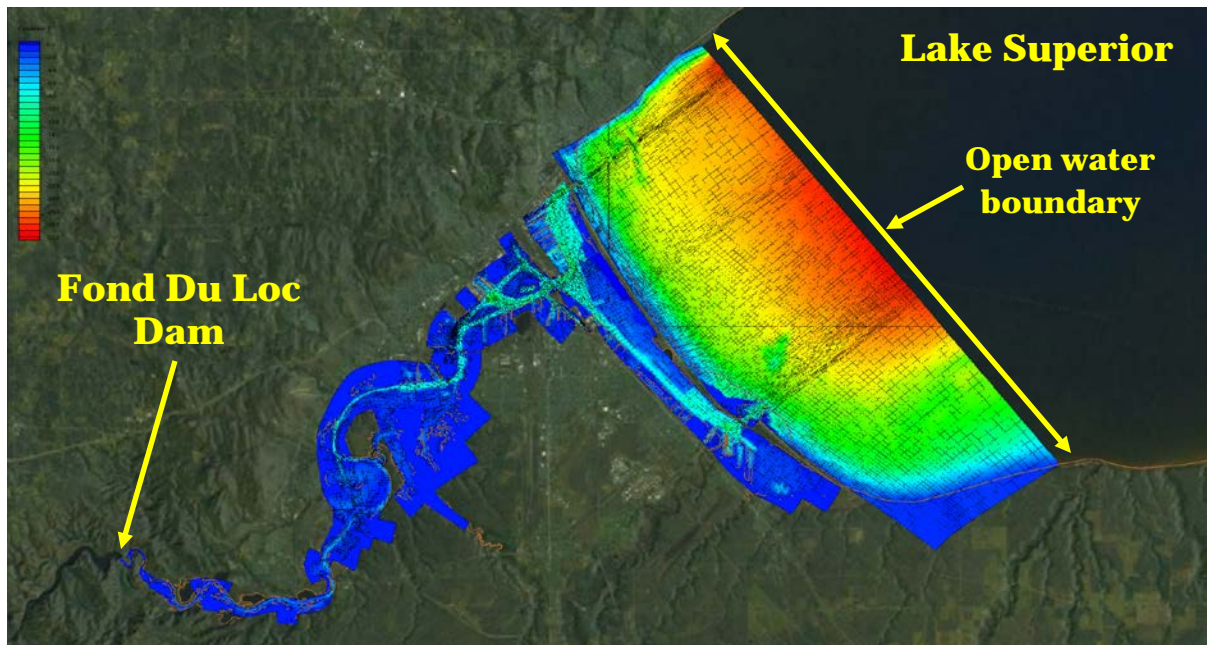


Figure 2-7 Model Domain for the DH-SLR GSMB model

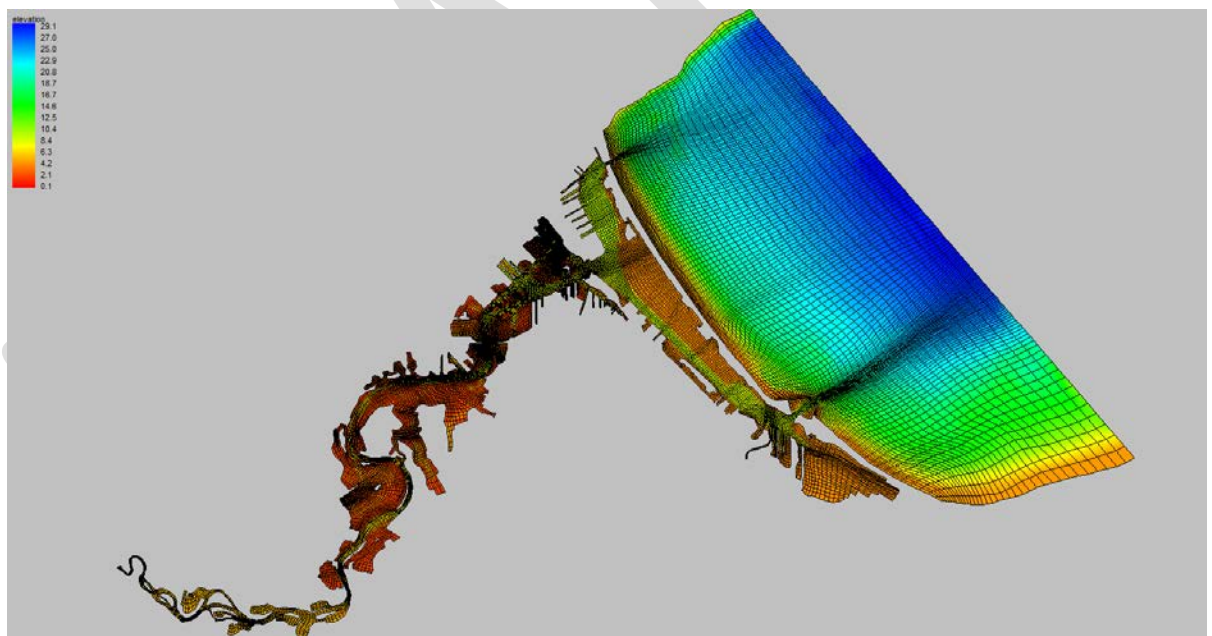


Figure 2-8 Initial Single Block Grid

Other boundary forcings included in the GSMB were the flows in the St. Louis River (see Figure 2-2) and the Nemadji River (see Figure 2-12), the wind record measured at the NOAA 9099064 Duluth Harbor station (see Figure 2-13), and the discharges from the 7 ft (2.13 m) diameter outfall from the Western Lake Superior Sanitary District wastewater treatment facility (WLSSD) (see Figure 2-14). The flow

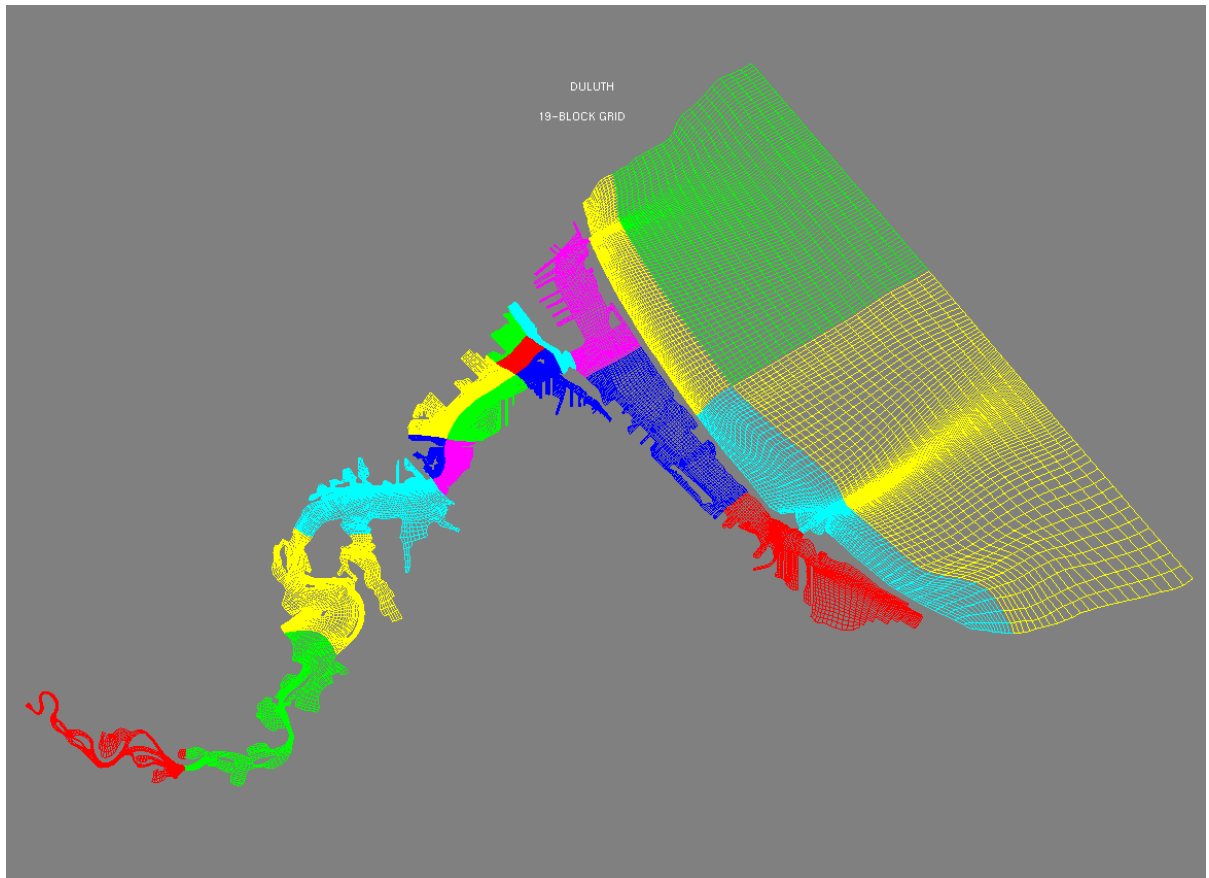


Figure 2-9 18-Block Grid of the DH-SLR Model Domain

measurements in the Nemadji River did not begin until mid-April in 2008. That is the reason for the linearly increasing flow in the first 25 days of the flow record plotted in Figure 2-12.

The GSMB Hydrodynamic module initially simulated the four month period 27 March – 26 July 2008 to insure there were no model instabilities or unrealistically high current velocities.

Depth (ft)

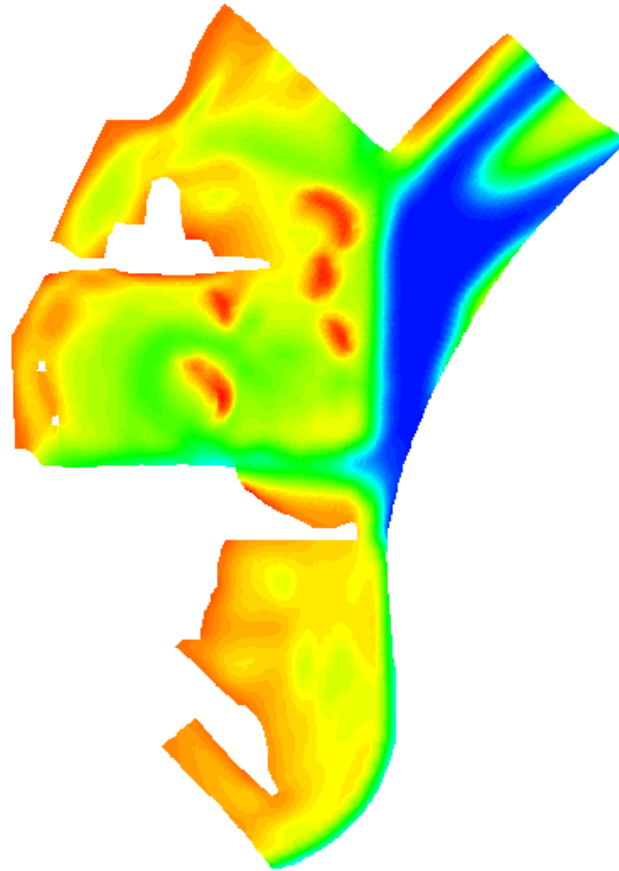
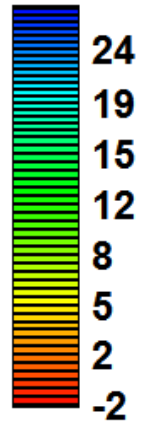


Figure 2-10 Block 5 with Shoals Design

DRY

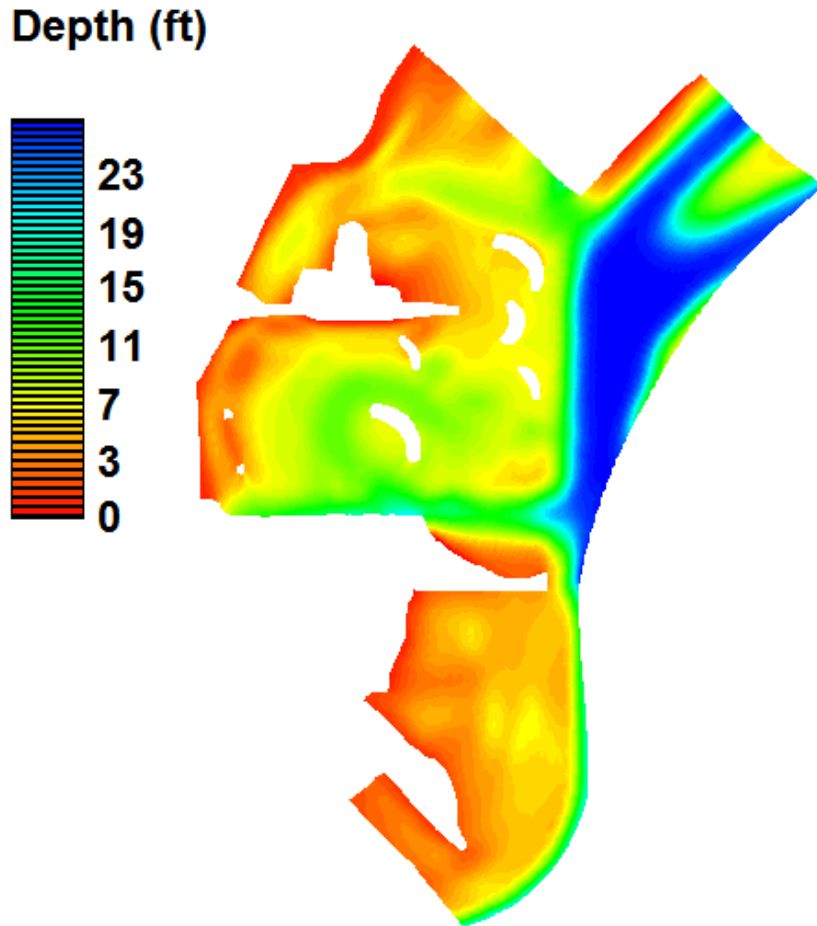


Figure 2-11 Block 5 with Island Design

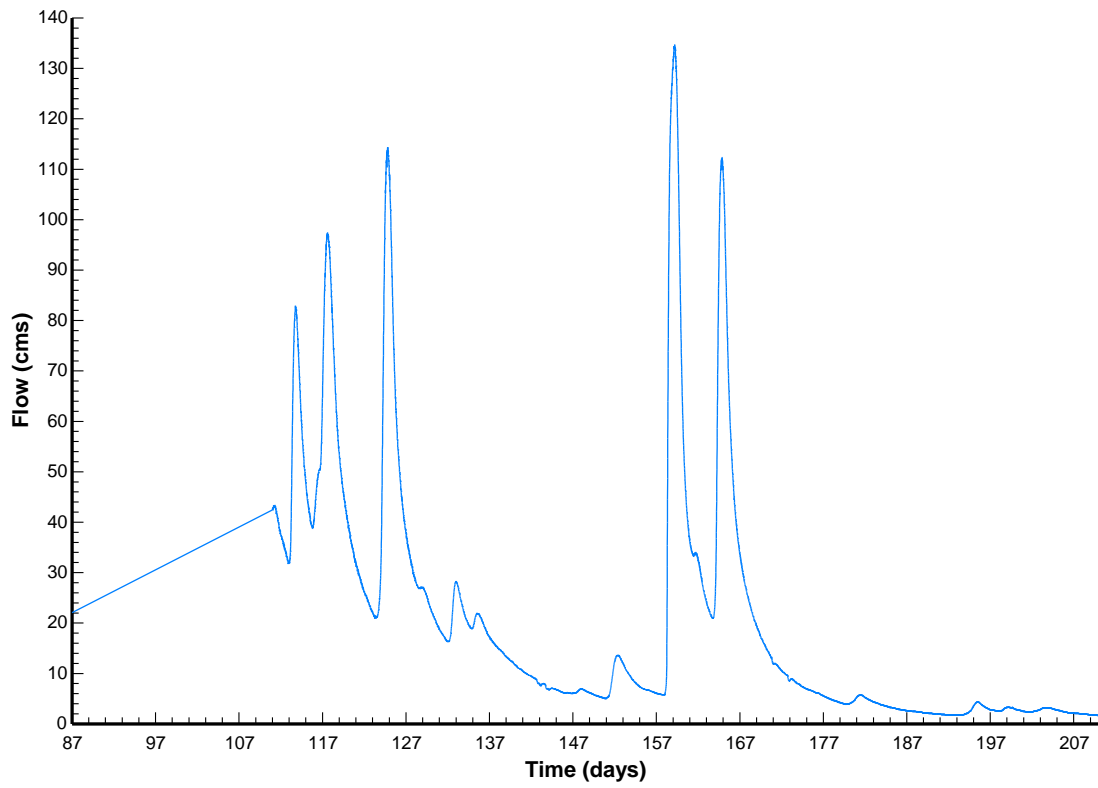


Figure 2-12 Nemadji River Flow Record (27-March-2008 through 26-July-2008)

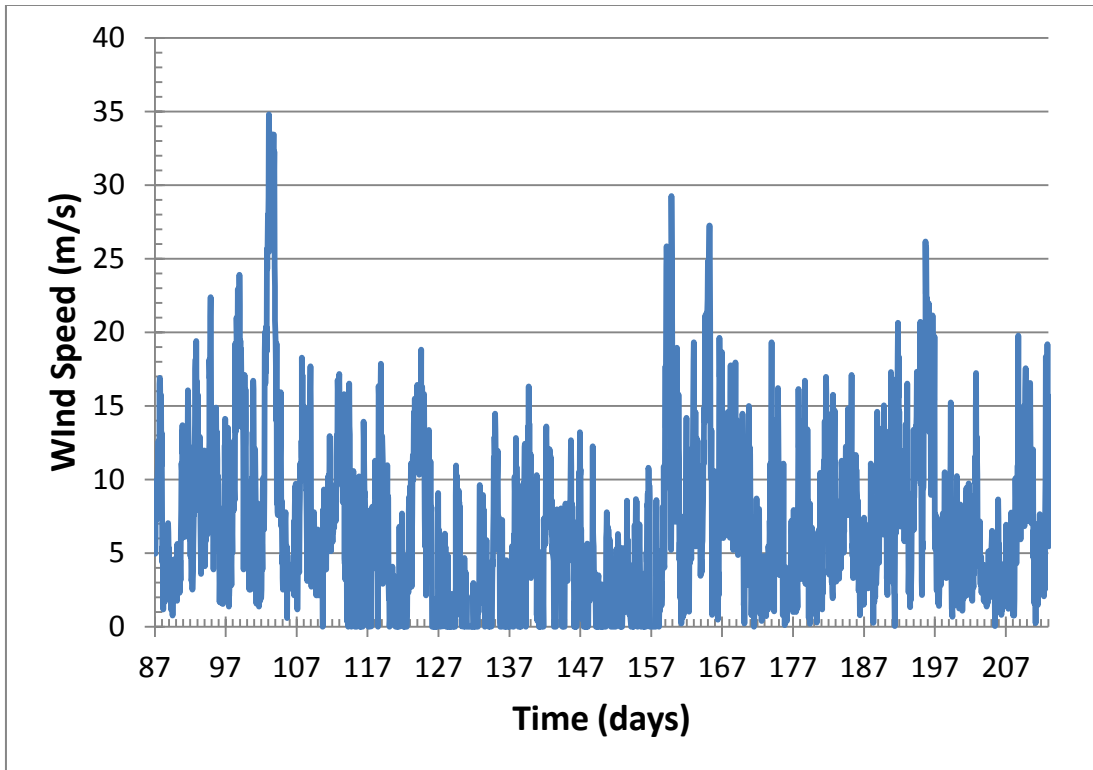


Figure 2-13a Wind Speed Record Measured at the Duluth NOAA Station (27-March-2008 through 26-July-2008)

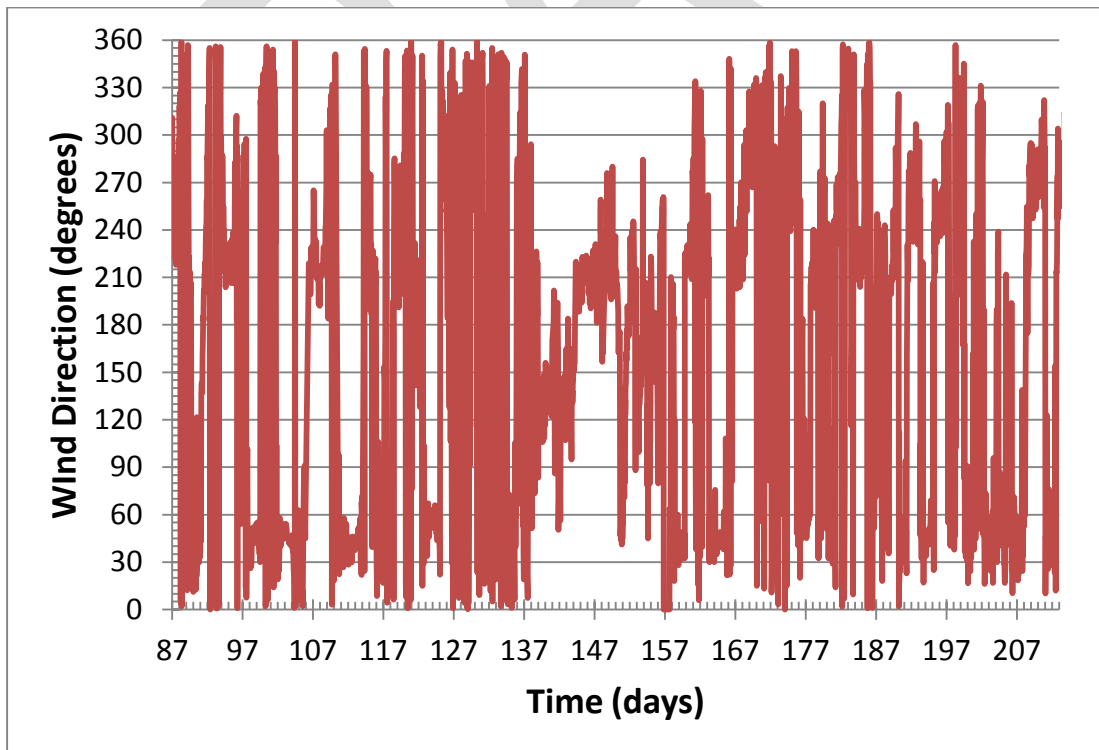


Figure 2-13b Wind Direction Record Measured at the Duluth NOAA Station (27-March-2008 through 26-July-2008)

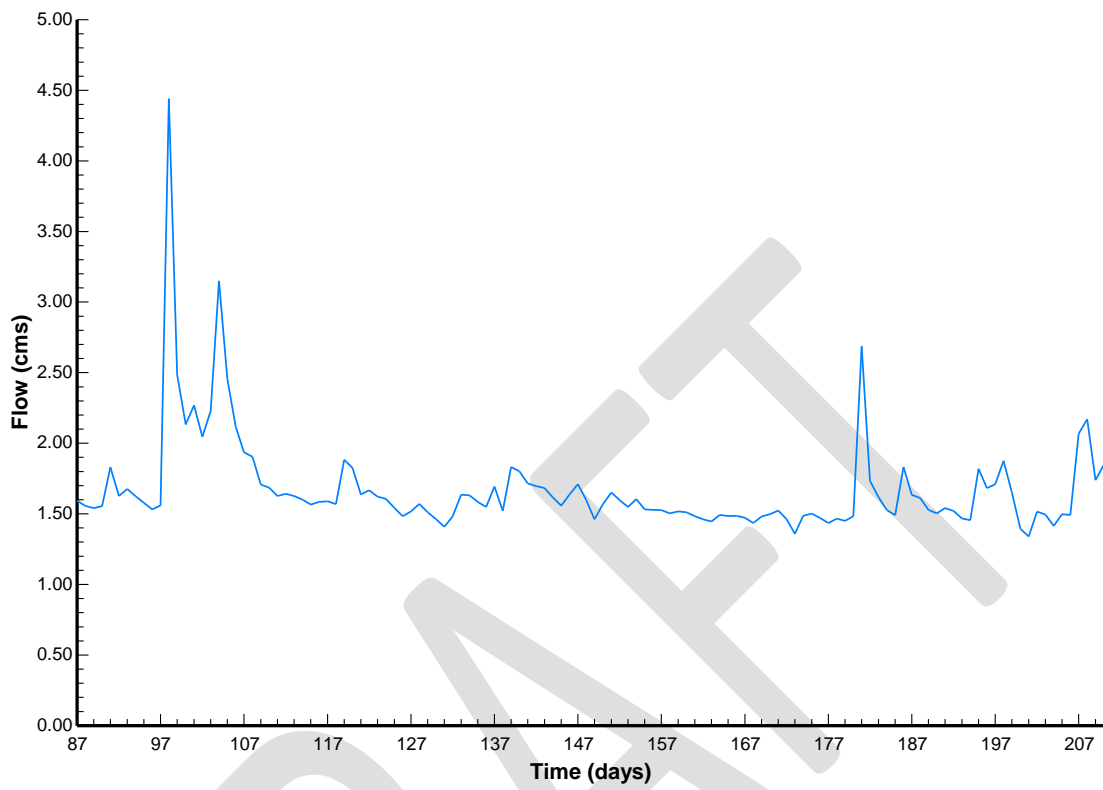


Figure 2-14 WLSSD Daily Average Discharges (27-March-2008 through 26-July-2008)

3 Wave Modeling

Purpose

Wave heights, periods, and directions are required for the GSMB model simulations. Nearshore wave modeling was performed to simulate wave generation and growth in St Louis River estuary for both the shoals and islands designs at the 40th Ave AOC. The surface wind and water level data collected at NOAA Coastal Stations 9099064 (Duluth, MN) was used as driving force for the wave modeling.

Wave Model

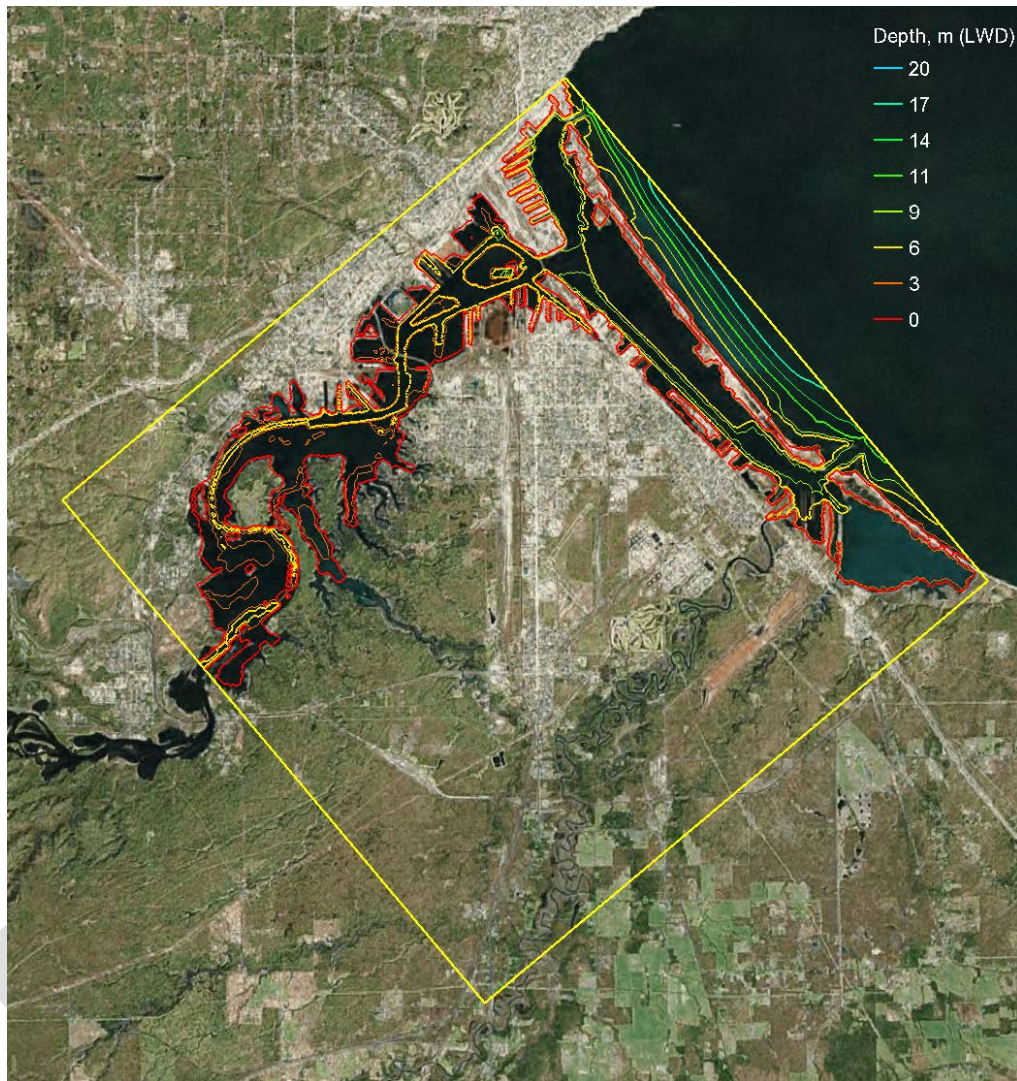
Wave modeling was conducted using CMS-Wave, a steady-state 2D spectral wave model (Lin *et al.* 2008; Lin *et al.* 2011a, 2011b) capable of simulating wave processes including wave generation and growth with ambient currents at coastal inlets and navigation channels. It is based on the wave-action balance equation that includes wave propagation, refraction, shoaling, diffraction, reflection, breaking, and dissipation. CMS-Wave is part of an integrated Coastal Modeling System (CMS) (Demirbilek and Rosati 2011) developed at ERDC-CHL to assist in coastal region project applications. CMS-Wave uses the Surface-water Modeling System (SMS) (Demirbilek *et al.* 2007; Zundel 2006) interface for grid generation, model setup, and post-processing. A more detailed description of CMS and CMS-Wave is given in Appendix A.

Model Setup

Model Grid

The CMS-Wave model grid covers a square area of 9.32 mi x 9.32 mi (15 km x 15 km). It is a non-uniform Cartesian grid with varying grid cell size from 1,076 ft² (100 m²) to 106,294 ft² (9,875 m²). The model bathymetry is the same as used in the CH3D-MB model. Figure 3-1 shows the CMS-Wave model domain and bathymetry contours.

Figure 3-1. CMS-Wave model domain and depth contours.



Forcing Conditions

The waves in the St Louis River estuary are mainly generated by the surface wind. Large wave conditions generally occur during strong wind and high water level. The local wind comes more from NE, SW, NW, and sometimes from the W direction. Average wind speeds of 20 knots or less are commonly observed in the area. Winter winds remain strong and come mostly out of the S through NW directions, and with an increase in northerlies.

The local water surface is subject to a consistent seasonal rise and fall. The lowest stage usually occurs in the late winter (February/March) and the highest in the late

summer (August/September). Strong northeasters in the winter can produce high water and large waves in Duluth Harbor.

The hourly wind and water level record measured at the Duluth NOAA 9099064 station was used to drive the CMS-Wave model. Figures 3-2 and 3-3 show the hourly measured wind and water levels, respectively, from NOAA 9099064 for March to July 2008.

Figure 3-2. NOAA Station 9099064 wind data for March to July 2008.

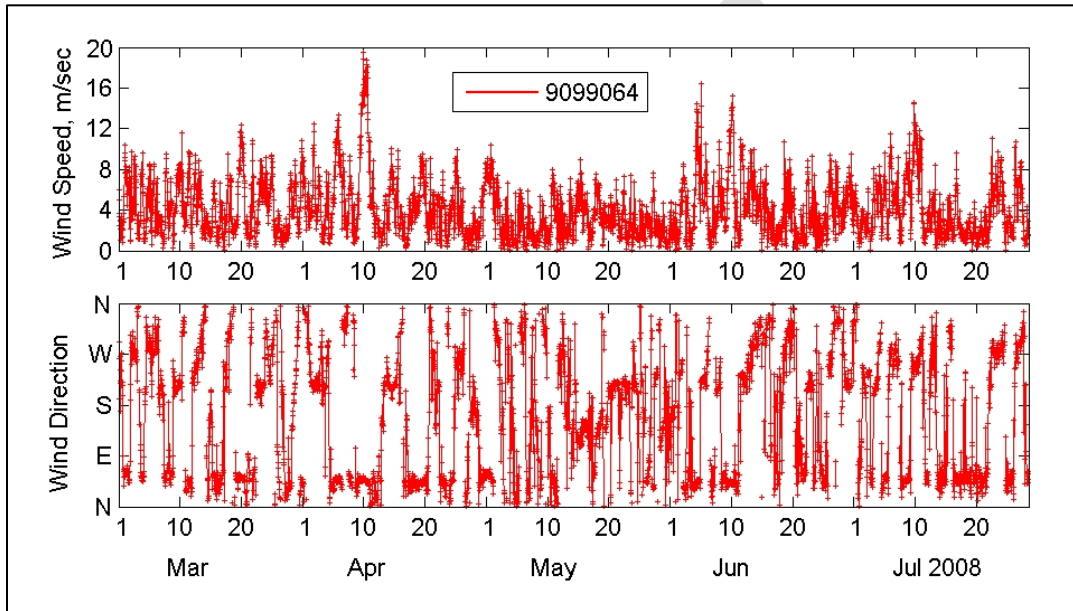
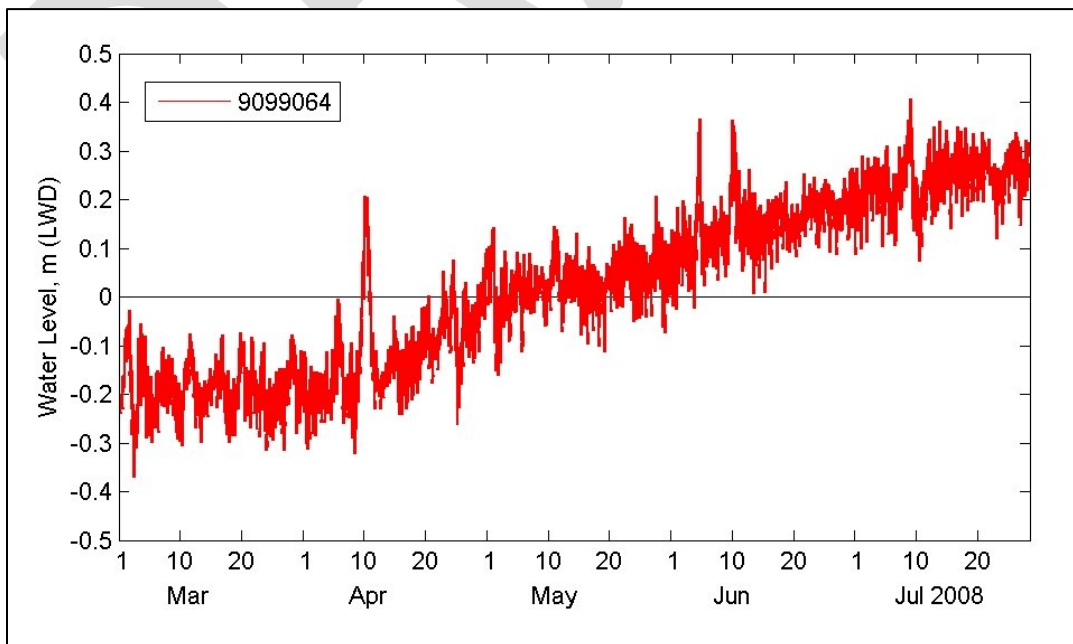


Figure 3-3. NOAA Station 9099064 Water level data for March to July 2008.



Model Simulations

Wave simulations were conducted for a four-month period from April to July 2008. Two four-month simulations were performed, one for the shoals design and the other for the islands design at the 40th Ave AOC. The time series of simulated wave properties (*i.e.*, heights, periods, and directions) for each of the two models were interpolated from the non-uniform Cartesian grid used by CMS-Wave to the curvilinear grid used by the CH3D-SEDZLJ model. The two time series of interpolated wave properties were used by the CH3D-SEDZLJ model to calculate the wave- and current-induced bed shear stress in each grid cell for every timestep during the four-month simulation. Figures 3-4 and 3-5 show two calculated wave fields encompassing the 40th Ave AOC corresponding to strong NE wind (40 kt) occurred at 0200 GMT 11th April and strong SW wind (34 kt) at 2100 GMT 6th June 2008, respectively.

Figure 3-4. Calculated wave field, 0200 GMT 11th April 2008.

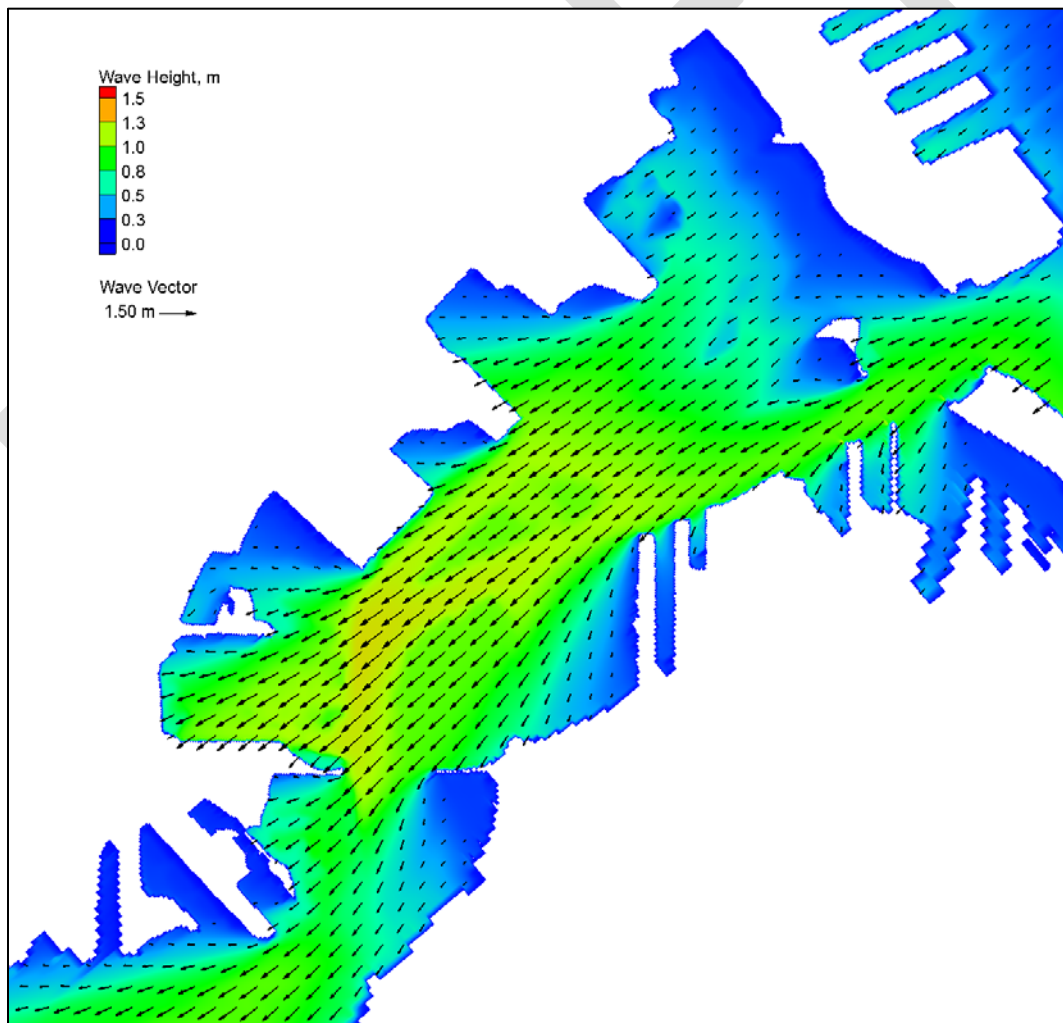
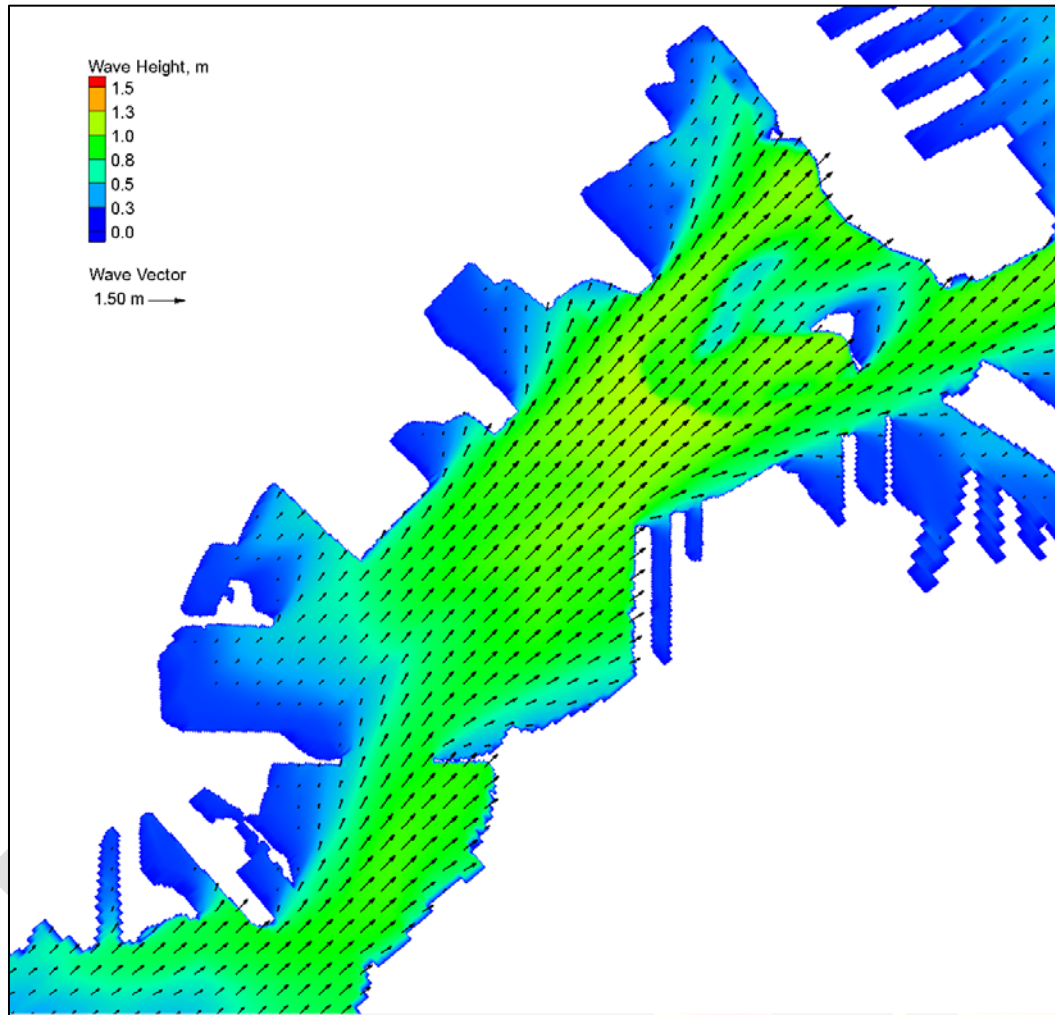


Figure 3-5. Calculated wave field, 2100 GMT 6th June 2008.



4 Sediment Transport Modeling

The sediment transport model in GSMB is the SEDZLJ sediment transport model (Jones and Lick 2001; James *et al.* 2010). SEDZLJ is an advanced sediment bed model that represents the dynamic processes of erosion, bedload transport, bed sorting, armoring, consolidation of fine-grain sediment dominated sediment beds, settling of flocculated cohesive sediment, settling of individual noncohesive sediment particles, and deposition. SEDZLJ is dynamically linked to CH3D-MB in that the hydrodynamics and sediment transport modules are run during each model time step. A description of SEDZLJ is given in Appendix B. SEDZLJ is not capable of simulating ice-induced sediment transport.

Setup of SEDZLJ

The SEDZLJ sediment model was setup to simulate sediment transport in the GSMB model domain seen in Figure 2-7 using the available sediment data (grain size distributions) for the dredged material to be placed in the 40th Ave AOC and the available grain size distribution data at other locations in the model domain. These sediment data were provided by LRE. One of the first steps in performing sediment transport modeling is to use these data from the site to determine how many discrete sediment size classes are needed to adequately represent the full range of sediment sizes. Typically, five to ten size classes are used. For the current modeling study five sediment size classes were used to represent the grain size distribution of the placed dredged material, and four sediment size classes were used to represent the native sediment. Each sediment size class is represented in SEDZLJ using the median or mean diameter within that size range. The five placed material sizes were 15, 100, 180, 425, and 850 μm , and the four native sediment size classes were 15, 200, 400, and 3,000 μm . The classifications of the five placed dredged material size classes are fine silt, very fine sand, fine sand, medium sand, and coarse sand. The classifications of the four native sediment size classes are fine silt, fine sand, medium sand, and very fine gravel. The specific gravity of all nine sediment size classes was assumed to be 2.65. The settling velocities for the eight different sediment sizes (there are only eight sediment sizes since the 15 μm size was used twice) were determined using Eq. B-2 (see Appendix B), and are shown in Table 4-1 below. The deposition rate for a particular size class was determined by multiplying the settling velocity by the suspended sediment concentration of that size class. The probabilities of deposition for all size classes were set equal to one (Mehta 2014).

Table 4-1 Settling Velocities of the Eight Modeled Sediment Sizes

<i>D</i> ₅₀ (μm)	<i>W</i> _s (mm/s)
15	0.10
100	5.97
180	16.2
200	19.1
400	47.3
425	50.6
850	97.1
3,000	228.8

The erosion rates of the four native sediment size classes were determined using the results obtained by Roberts *et al.* (1998) who measured the erosion rates of quartz particles in a SEDFLUME. SEDFLUME is a field- or laboratory-deployable flume for measuring the erosion rates of cohesive and noncohesive sediment beds (McNeil *et al.* 1996). The erosion rates for the five placed dredged material sediment size classes were determined using the results from SEDFLUME tests performed on placed sediment samples collected at the 21st Ave W placement sites and shipped to ERDC-CHL for analysis. The erosion rates for the consolidated sediment in the SEDFLUME tests were used in the modeling since it was assumed that the placed dredged material would undergo fairly rapid consolidation following placement.

Spatially varying composition of the sediment bed in the 18 grid blocks in the GSMB model was specified as initial bed properties using the available sediment data. Grid block 5 is where the 40th Ave AOC is located, so the sediment composition in that grid block contained both native and placed dredged material. The grain size distributions for the four native sediment size classes and for the five placed sediment size classes are shown in Table 4-2. Each number in this table represents the percentage of each of the 9 sediment size classes for the two sediment types in the top bed layer. The first two size classes shown in this table represent fine size silts for native sediment and the placed dredged material, respectively. As instructed by LRE, the composition of the placed dredged material was specified as 50% fine-grain sediment and 50% non-cohesive sediment. As seen in Table 4-2, the placed

Table 4-2 Percentages of Sediment Size Classes for Sediment Types

Sediment Type	Sediment Size Class (and sizes)								
	1 (15 μm)	2 (15 μm)	3 (200 μm)	4 (400 μm)	5 (3000 μm)	6 (100 μm)	7 (180 μm)	8 (425 μm)	9 (850 μm)
Native Sediment	30	0	30	30	10	0	0	0	0
Placed Sediment	0	50	0	0	0	24	24	1	1

material was represented by size classes 2, 6, 7, 8, and 9, and the percentages of these size classes in the sediment bed layers were 50, 24, 24, 1, and 1 percent, respectively. Note that these five percentages add up to 100 percent. Likewise, the native sediment was represented by size classes 1, 3, 4, and 5, and the percentages of these size classes in the sediment bed layers were 30, 30, 30, and 10 percent, respectively.

The existing sediment bed in each grid cell was divided into four vertical layers (see Figure B-2). The assumption was made that the initial distribution of the 9 size classes, bulk densities, and gross erosion rates are the same in all four bed layers, *i.e.*, there is no initial vertical stratification of sediment grain sizes, bulk densities or erosion rates that normally result from the repetitive processes of deposition, erosion, and armoring of the top bed layer.

Modeling Results

Results from the four month simulation for the shoals design are shown in Figures 4-1 and 4-2. These are color contour plots of the net negative (*i.e.*, erosion) change in bed elevation at the end of the simulation period. Net deposition occurs in the uncolored cells. Figure 4-2 is a zoomed in view of the area in proximity to the shoals, and also shows the outline of the shoals in black. As seen in this figure, there is minimal net erosion on top of and around the shoals. This result is not unexpected

due to the shallow depths above and around the shoals. Figure 4-1 shows that the maximum net erosion depth was approximately 24 cm (0.8 ft). Net erosion does not mean that deposition is not simulated to occur in these grid cells. It means that more erosion is predicted to occur than erosion over the four month simulation. The bed elevation decreases, and therefore the flow depth increases in a grid cell in which net erosion is simulated to occur.

Results from the four month simulation for the islands design is shown in Figure 4-3. This color contour plots of the change in bed elevation at the end of the simulation period. The blue to green colors in this figure indicate locations where net erosion is predicted to occur. As seen, these areas are mostly in shallow waters around the islands and along exposed shorelines. The maximum net erosion depth in the area in proximity to the islands was approximately 25 cm (0.82 ft). No net erosion occurred on the exposed side of the three outer islands because the water depth is greater than 6.6 ft (2 m) adjacent to these islands. This depth minimized the wave contribution to the bed shear stress due to the short period of the locally generated waves. In turn, this minimized the amount of erosion that occurred at these locations, and resulted in minimal net deposition occurring over the four month simulation.

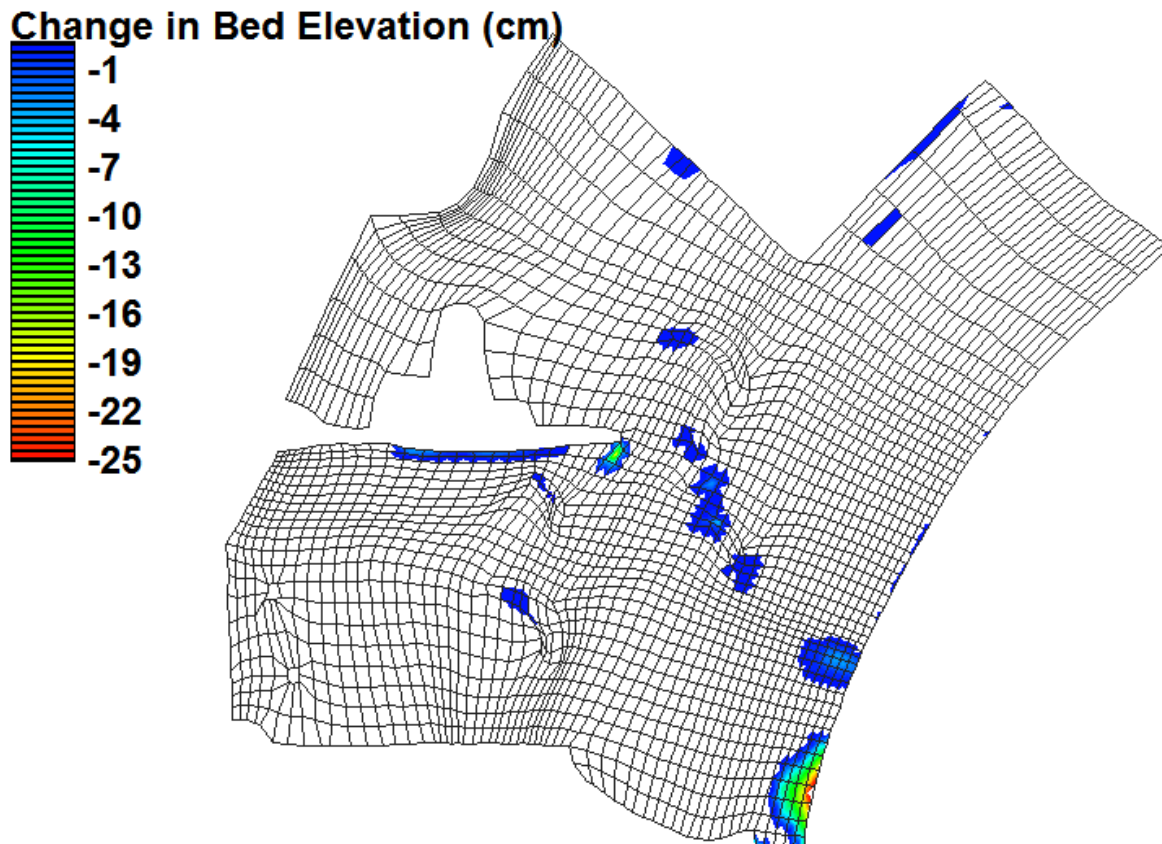


Figure 4-1 Color contoured plot of the net negative change in bed elevation in Block 5 for the shoals design.

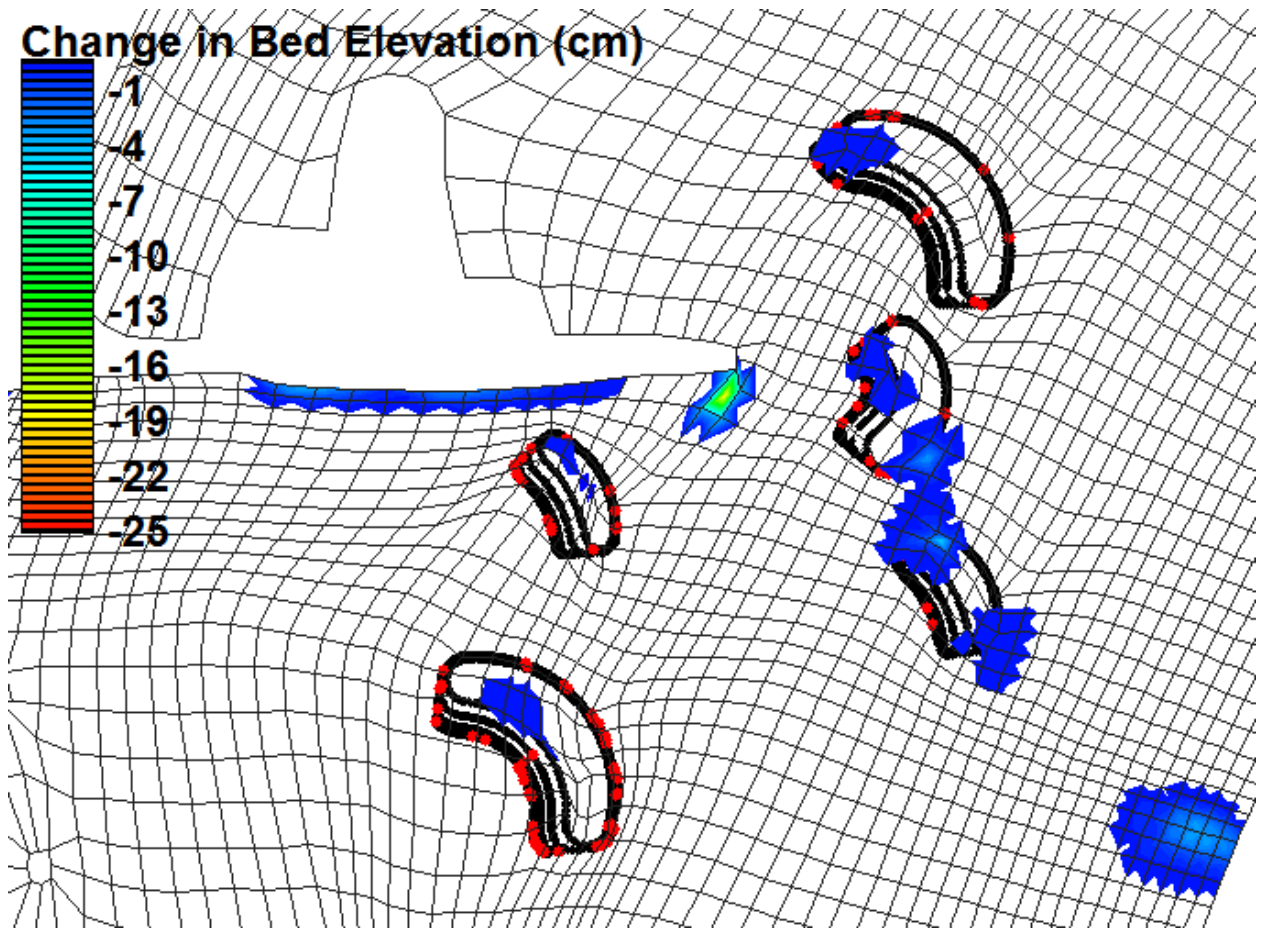


Figure 4-2 Zoomed in color contoured plot of the net negative change in bed elevation in Block 5 and the shapes of the designed shoals.

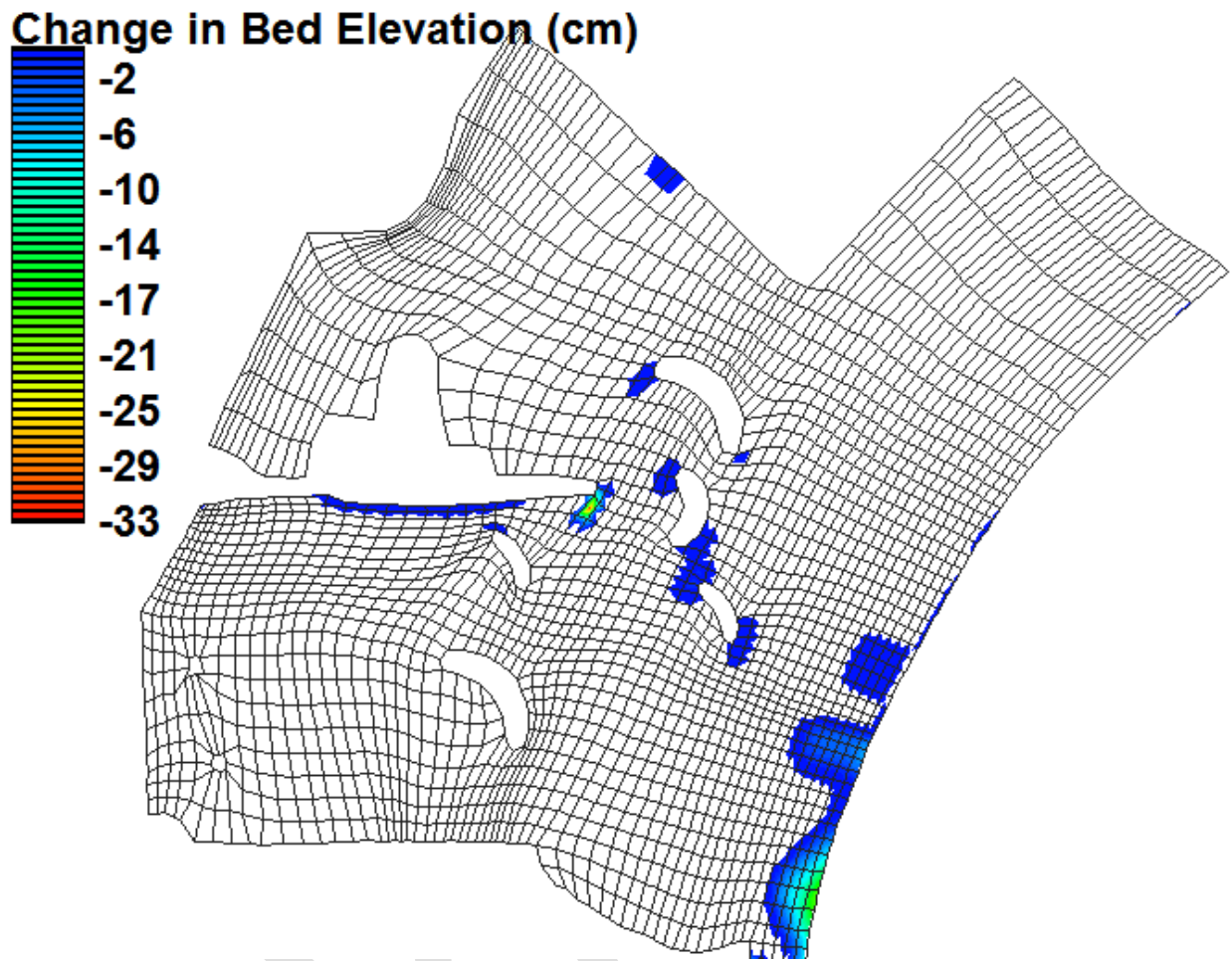


Figure 4-3 Color contoured plot of the net negative change in bed elevation in Block 5 for the islands design.

5 Conclusions

Model simulations of the transport of both native sediment and placed dredged material over the selected four-month period (27 March – 26 July 2008) were performed for both the shoals and islands features designed for the 40th Ave AOC using the GSMB hydrodynamic and mixed sediment transport model. The main conclusion from the modeling for both designs is that minimal net erosion occurred over the simulated four-month period. The following two factors contribute jointly to this:

- As previously mentioned, the short period wind waves that are generated inside the harbor do not affect the calculated bed shear stresses unless the water depths are fairly shallow. This reduces the areas where erosion occurs.
- The 40th Ave embayment is off the main channel/river, so the flows in this area, that are the result of wind generated circulation as well as circulation resulting from flow separation off the point of land immediately to the south of this embayment, are low except during large storm events. These low flows also contribute to the relatively small amount of net erosion that occurs.

References

- Arega, F., and E.J. Hayter. 2008. "Coupled consolidation and contaminant transport model for simulating migration of contaminants through sediment and a cap," *Journal of Applied Mathematical Modelling*, 32:2413–2428.
- Bunch, B.W., M. Channel, W.D. Corson, B.A. Ebersole, L. Lin, D.J. Mark, J.P. McKinney, S.A. Pranger, P.R. Schroeder, S.J. Smith, D.H. Tillman, B.A. Tracy, M.W. Tubman, and T.L. Welp. 2003. "Evaluation of Island and Nearshore Confined Disposal Facility Alternatives, Pascagoula River Harbor Dredged Material Management Plan," Technical Report ERDC-03-3, U.S. Army Engineer Research and Development Center, Vicksburg, MS.
- Cerco, C., and T. Cole. 1994. "Three-Dimensional Eutrophication Model of Chesapeake Bay," Technical Report EL-94-4, U.S. Army Engineer Waterways Experiment Station, Vicksburg, MS.
- Chapman, R.S., B.H. Johnson, and S.R. Vemulakonda. 1996. "User guide for the sigma stretched version of CH3D-WES; A three-dimensional numerical hydrodynamic, salinity and temperature model," Technical Report HL-96-21, U.S. Army Engineer Waterways Experiment Station, Vicksburg, MS.
- Chapman, R.S., P.V. Luong, and M.W. Tubman. 2006. "Mississippi Sound hydrodynamic and salinity sensitivity modeling," Final Report prepared for U.S. Army District, Mobile, AL.
- Chapman, R. S., and P.V. Luong. 2009. "Development of a multi-block CH3D with a wetting, drying and CLEAR linkage capability," Draft Report prepared for Louisiana Coastal Area (LCA) Ecosystem Restoration Plan S&T Office, Vicksburg, MS.
- Chapman, R.S., K.J. Eisses, and T.O. McAlpin. 2010. "Numerical modeling studies supporting Port of Anchorage deepening and expansion; part iii: numerical hydrodynamic modeling," *Proceedings 11th International Conference on Estuarine and Coastal Modeling*, November 4-6, 2010, Seattle, WA, 301-316.
- Chapman, R.S., A.S. Grzegorzewski, P.V. Luong, E.R. Smith, S.J. Smith, and M.W. Tubman. 2011. "The Effects of DA-10 Removal on Circulation and Sediment Transport Potential within the Horn Island Pass and Lower Pascagoula Sound Channels," Final Report prepared for U. S. Army District, Mobile, AL.
- Chapman R.S, E.J. Hayter, S.J. Smith, P.V. Luong, M. Tubman, A.S. Grzegorzewski, J.Z. Gailani, B.W. Bunch, D.H. Tillman. 2012. "Hydrodynamic, Water Quality

- and Sediment Transport Modeling to Investigate the Impacts of Widening the Pascagoula Lower Sound and Bayou Casotte Navigation Channels,” Final Report prepared for U. S. Army District, Mobile, AL.
- Cheng, N.S. 1997. “Simplified settling velocity formula for sediment particles,” *Journal of Hydraulic Engineering*, 123(2):149-152.
- Demirbilek, Z., L. Lin, and A. Zundel. 2007. “WABED model in the SMS: Part 2. Graphical interface,” Coastal and Hydraulics Laboratory Engineering Technical Note ERDC/CHL CHETN-I-74. Vicksburg, MS: U.S. Army Engineer Research and Development Center.
- Demirbilek, Z. and J.D. Rosati. 2011. “Verification and validation of the Coastal Modeling System, Report 1: Summary Report,” ERDC/CHL Technical Report 11-10, U.S. Army Corps of Engineers Research and Development Center, Vicksburg, MS.
- Hayter, E.J., and S.J. Smith. 2010. “Numerical modeling studies supporting Port of Anchorage deepening and expansion - part iv; Numerical Sediment Transport Modeling,” *Proceedings 11th International Conference on Estuarine and Coastal Modeling*, November 4-6, 2010, Seattle, WA, 317-332.
- Hayter E.J., R.S. Chapman, P.V. Luong, S.J. Smith, and D.B. Bryant. 2012. “Demonstration of Predictive Capabilities for Fine-Scale Sedimentation Patterns within the Port of Anchorage, AK,” Letter Report prepared for U.S. Army District, Anchorage, AK.
- James, S.C., C.A. Jones, M.D. Grace, and J.D. Roberts. 2010. “Advances in sediment transport modelling,” *Journal of Hydraulic Research*, 48: 6, 754-763.
- Jensen, R.E., Cialone, M.A., Chapman, R. S., Ebersole, B. E., Anderson, M. and L. Thomas, 2012. “Modeling of Lake Michigan Storm Waves and Water Levels.,” Technical Report for the U.S. Army Engineer District, Detroit by the U.S. Army Engineer Research and Development Center, Vicksburg, MS.
- Jones, C.A., and W. Lick. 2001. “SEDZLJ: A sediment transport model,” Final Report. University of California, Santa Barbara, California.
- Lin, L., Z. Demirbilek, H. Mase, J. Zheng, and F. Yamada. 2008. “CMS-Wave: A Nearshore Spectral Wave Processes Model for Coastal Inlets and Navigation Projects,” U.S. Army Engineer Research and Development Center Technical Report ERDC-CHL TR-08-13. Vicksburg, MS.
- Lin, L., Z. Demirbilek, and H. Mase. 2011a. “Recent capabilities of CMS-Wave: A coastal wave model for inlets and navigation projects,” Proceedings, Symposium to honor Dr. Nicholas Kraus. *Journal of Coastal Research*,

Special Issue 59, 7-14.

- Lin, L., Z. Demirbilek, R. Thomas, and J. Rosati. 2011b. "Verification and validation of the Coastal Modeling System, Report 2: CMS-Wave," ERDC/CHL Technical Report 11-10, U.S. Army Corps of Engineers Research and Development Center, Vicksburg, MS.
- Luong, P.V., and R.S. Chapman, 2009. "Application of Multi-block Grid and Parallelization Techniques in Hydrodynamic Modeling, DOD High Performance Computing Modernization Program: User Group Conference (HPCMP-UGC), San Diego, CA.
- Mausolf, G.M. 2014. "Numerical Modeling and Sediment Transport Analysis for 21st Ave West Section 204 Study in St. Louis Bay off Lake Superior in Duluth, WI," Hydraulics and Hydrology Technical Memorandum, U.S. Army Corps of Engineers, Detroit District, Detroit, MI.
- McNeil, J., C. Taylor, and W. Lick. 1996. "Measurements of the erosion of undisturbed bottom sediments with depth." *Journal of Hydraulic Engineering*, 122(6):316-324.
- Mehta, A.J. 2014. *An introduction to hydraulics of fine sediment transport*. Advanced series on Ocean Engineering: Volume 38. Hackensack, NJ: World Scientific.
- Smith, J.M., D.T. Resio, and A. Zundel. 1999. "STWAVE: Steady-state spectral wave model, Report 1: User's manual for STWAVE Version 2.0," Coastal and Hydraulics Laboratory Instruction Report CHL-99-1, Vicksburg, MS: U.S. Army Engineer Waterways Experiment Station.
- Snir, M., S. Otto, S. Huss-Lederman, D. Walker, and J. Dongarra. 1998. "MPI - The Complete Reference: Volume 1, the MPI Core," MIT Press, Cambridge, MA.
- STARR. 2012. "Great Lakes Storm Surge Analysis Lake Superior, FEMA Region V, Technical Support Data Notebook," Contract No. HSFEHQ-09-D-0370, Task Order No. HSFE05-10-J-0007.
- Sanford, L.P. 2008. "Modeling a dynamically varying mixed sediment bed with erosion, deposition, bioturbation, consolidation, and armoring," *Computers & Geosciences*, 34(10):1263-1283.
- Smith, S.J., R.S. Chapman, D.J. Mark, and T.O. MacAlpin. 2008. "Hydrodynamic evaluation of proposed the Port of Anchorage expansion," Draft Report to POA, U.S. Army Engineer Waterways Experiment Station, Vicksburg, MS.

Smith, S.J., M.D. Peterson, and T.C. Pratt. 2010. "Numerical modeling studies supporting Port of Anchorage deepening and expansion; part ii: measuring physical processes," *Proceedings 11th International Conference on Estuarine and Coastal Modeling*, November 4-6, 2009, Seattle, WA. 286-300.

Snir, M., S. Otto, S. Huss-Lederman, D. Walker, and J. Dongarra. 1998. "MPI - The Complete Reference: Volume 1, the MPI Core," MIT Press, Cambridge, MA.

Van Rijn, L.C. 1984. "Sediment Transport: part i: bedload transport; part ii: suspended load transport; part iii: bed forms and alluvial roughness," *Journal of Hydraulic Engineering*, 110(10): 1431-1456; 110(11): 1613-1641, 110(12): 1733-1754.

Zundel, A. K. (2006). "Surface-water modeling system reference manual – Version 9.2," Provo, UT: Brigham Young University Environmental Modeling Research Laboratory.

DRAFT

Appendix A

Description of CMS-Wave

The Coastal Modeling System (CMS) was used for the numerical modeling estimates of waves, currents, and sediment transport at the Canaveral Harbor ODMDS. A brief description of the CMS is provided here for completeness.

As shown in Figure A-1, the CMS is an integrated suite of numerical models for waves, flows, and sediment transport and morphology change in coastal areas. This modeling system includes representation of relevant nearshore processes for practical applications of navigation channel performance, and sediment management at coastal inlets and adjacent beaches. The development and enhancement of CMS capabilities continues to evolve as a research and engineering tool for desk-top computers. CMS uses the Surface-water Modeling System (SMS; Zundel 2006) interface for grid generation and model setup, as well as plotting and post-processing. The Verification and Validation (V&V) Report 1 (Demirbilek and Rosati 2011) and Report 2 (Lin *et al.* 2011) have detailed information about the CMS-Wave features, and evaluation of model's performance skills in a variety of applications. Report 3 and Report 4 in the V&V series describe coupling of wave-flow models and hydrodynamic and sediment transport and morphology change aspects of CMS-Flow. The performance of CMS for a number of applications is summarized in Report 1 and details are described in the three companion V&V Reports 2 - 4.

The CMS-Wave, a spectral wave model, is used in this study given the large extent of modeling domain over which wave estimates were required. Wind wave generation and growth, diffraction, reflection, dissipation due to bottom friction, white-capping and breaking, wave-current interaction, wave run-up, wave setup, and wave transmission through structures are the main wave processes included in the CMS-Wave.

CMS-Wave model solves the steady-state wave-action balance equation on a non-uniform Cartesian grid to simulate steady-state spectral transformation of directional random waves. CMS-Wave is designed to simulate wave processes with ambient currents at coastal inlets and in navigation channels. The model can be used either in half-plane or full-plane mode for spectral wave transformation (Lin *et*

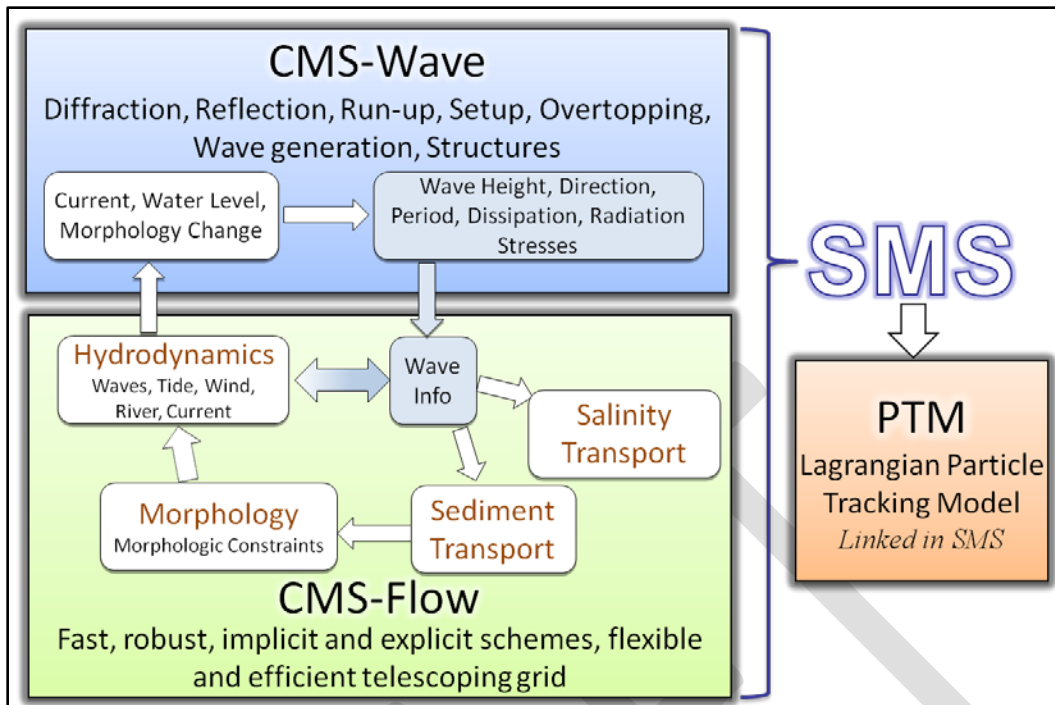


Figure A-1. The CMS framework and its components.

al. 2008; Demirbilek *et al.* 2007). The half-plane mode is default because in this mode CMS-Wave can run more efficiently as waves are transformed primarily from the seaward boundary toward shore. See Lin *et al.* (2011 and 2008) for features of the model and step-by-step instructions with examples for application of CMS-Wave to a variety of coastal inlets, ports, structures, and other navigation problems. Publications listed in the V&V reports and this report provide additional information about the CMS-Wave and its engineering applications. Additional information about CMS-Wave is available from the CIRP website: <http://cirp.usace.army.mil/wiki/CMS-Wave>

The CMS-Flow, a two-dimensional shallow-water wave model, was used for hydrodynamic modeling (calculation of water level and current) in this study. The implicit solver of the flow model was used in this study. This circulation model provides estimates of water level and current given the tides, winds, and river flows as boundary conditions. CMS-Flow calculates hydrodynamic (depth-averaged circulation), sediment transport and morphology change, and salinity due to tides, winds and waves.

The hydrodynamic model solves the conservative form of the shallow water equations that includes terms for the Coriolis force, wind stress, wave stress, bottom stress, vegetation flow drag, bottom friction, wave roller, and turbulent diffusion. Governing equations are solved using the finite volume method on a non-uniform

Cartesian grid. Finite-volume methods are a class of discretization schemes, and this formulation is implemented in finite-difference for solving the governing equations of coastal wave, flow and sediment transport models. V&V Reports 3 & 4 by describe the preparation of flow model for coastal applications. Additional information about CMS-Flow is available from the CIRP website:

<http://cirp.usace.army.mil/wiki/CMS-Flow>

CMS-Flow modeling task included specification of winds and water levels to the model. The effects of waves on the circulation were input to the CMS-Flow and have been included in the simulations performed for this study.

There are three sediment transport models available in CMS-Flow: a sediment mass balance model, an equilibrium advection-diffusion model, and a non-equilibrium advection-diffusion model. Depth-averaged salinity transport is simulated with the standard advection-diffusion model and includes evaporation and precipitation. The V&V Report 1, Report 3 and Report 4 describe the integrated wave-flow-sediment transport and morphology change aspects of CMS-Flow. The performance of CMS-Flow is described for a number of applications in the V&V reports.

Appendix B

Description of SEDZLJ Sediment Transport Model

The sediment transport model in GSMB is the SEDZLJ sediment transport model (Jones and Lick 2001; James *et al.* 2010). SEDZLJ is dynamically linked to CH3D-MB in that the hydrodynamics and sediment transport modules are run during each model time step. A description of this sediment transport model is given next.

Suspended Load Transport of Sediment

The GSMB hydrodynamic module simulates the transport of each of the sediment classes to determine the suspension concentration for each size class in every water column layer in each grid cell. The transport of suspended sediment is determined through the solution of the following 3D advective-dispersive transport equation for each of the sediment size classes that is used in the model:

$$\frac{\partial C_i}{\partial t} + \frac{\partial u C_i}{\partial x} + \frac{\partial v C_i}{\partial y} + \frac{\partial (w - W_{Si}) C_i}{\partial z} = \frac{\partial}{\partial x} \left(K_H \frac{\partial C_i}{\partial x} \right) + \frac{\partial}{\partial y} \left(K_H \frac{\partial C_i}{\partial y} \right) + \frac{\partial}{\partial z} \left(K_V \frac{\partial C_i}{\partial z} \right) + S_i \quad (\text{B-1})$$

where C_i = concentration of i th size class of suspended sediment, (u, v, w) = velocities in the (x, y, z) directions, t = time, W_{Si} = settling velocity of i th sediment size class, K_H = horizontal turbulent eddy diffusivity coefficient, K_V = vertical turbulent eddy diffusivity coefficient, and S_i = source/sink term for the i th sediment size class that accounts for erosion/deposition.

The settling velocities for noncohesive sediments are calculated in SEDZLJ using the following equation (Cheng 1997):

$$W_s = \frac{\mu}{d} \left(\sqrt{25 + 1.2 d_*^2} - 5 \right)^{\frac{3}{2}} \quad (\text{B-2})$$

where μ = dynamic viscosity of water; d = sediment diameter; and d_* = non-dimensional particle diameter given by:

$$d_* = d \left[(\rho_s / \rho_w - 1) g / \nu^2 \right]^{1/3} \quad (\text{B-3})$$

where ρ_w = water density, ρ_s = sediment particle density, g = acceleration due to gravity, and ν = kinematic fluid viscosity. Cheng's formula is based on measured

settling speeds of real sediments. As a result it produces slower settling speeds than those given by Stokes' Law because real sediments have irregular shapes and thus a greater hydrodynamic resistance than perfect spheres as assumed in Stokes' law.

The erosion and deposition of each of the sediment size classes, *i.e.*, the source/sink term in the 3D transport equation given above, and the subsequent change in the composition and thickness of the sediment bed in each grid cell are calculated by SEDZLJ at each time step.

Description of SEDZLJ

SEDZLJ is an advanced sediment bed model that represents the dynamic processes of erosion, bedload transport, bed sorting, armoring, consolidation of fine-grain sediment dominated sediment beds, settling of flocculated cohesive sediment, settling of individual noncohesive sediment particles, and deposition. An active layer formulation is used to describe sediment bed interactions during simultaneous erosion and deposition. The active layer facilitates coarsening during the bed armoring process. The SEDZLJ model was designed to directly use the results obtained from a SEDFLUME study. A description of SEDFLUME is available at <http://chl.erd.c.usace.army.mil/CHL.aspx?p=s&a=ARTICLES;630>. SEDFLUME is a straight, closed conduit rectangular cross-section flume in which detailed measurements of critical shear stress of erosion and erosion rate as a function of sediment depth are made using sediment cores (dominated by cohesive or mixed sediments) that are collected at the site to be modeled (McNeil *et al.* 1996). However, when SEDFLUME results are not available, it is possible to use a combination of literature values for these parameters as well as the results of SEDFLUME tests performed at other similar sites. In this case, a detailed sensitivity analysis should be performed to assist in quantifying the uncertainty that results from the use of these non-site specific erosion parameters.

Figure B-1 shows the simulated sediment transport processes in SEDZLJ. In this figure, U = near bed flow velocity, C = near bed sediment concentration, δ_{bl} = thickness of layer in which bedload transport occurs, U_{bl} = average bedload transport velocity, D_{bl} = sediment deposition rate for the sediment being transported as bedload, E_{bl} = sediment erosion rate for the sediment being transported as bedload, E_{sus} = sediment erosion rate for the sediment that is eroded and entrained into suspension, and D_{sus} = sediment deposition rate for suspended sediment. Specific capabilities of SEDZLJ are listed below.

- Whereas a hydrodynamic model is calibrated to account for the total bed shear stress, which is the sum of the form drag due to bed forms and other large-scale

physical features (e.g., boulder size particles) and the skin friction (also called the surface friction), the correct component of the bed shear stress to use in predicting sediment resuspension and deposition is the skin friction. The skin friction is calculated in SEDZLJ as a function of the near-bed current velocity and the effective bed roughness. The latter is specified in SEDZLJ as a linear function of the mean particle diameter in the active layer.

- Multiple size classes of both fine-grain (*i.e.*, cohesive) and noncohesive sediments can be represented in the sediment bed. This capability is necessary in order to simulate coarsening and subsequent armoring of the surficial sediment bed surface during high flow events.

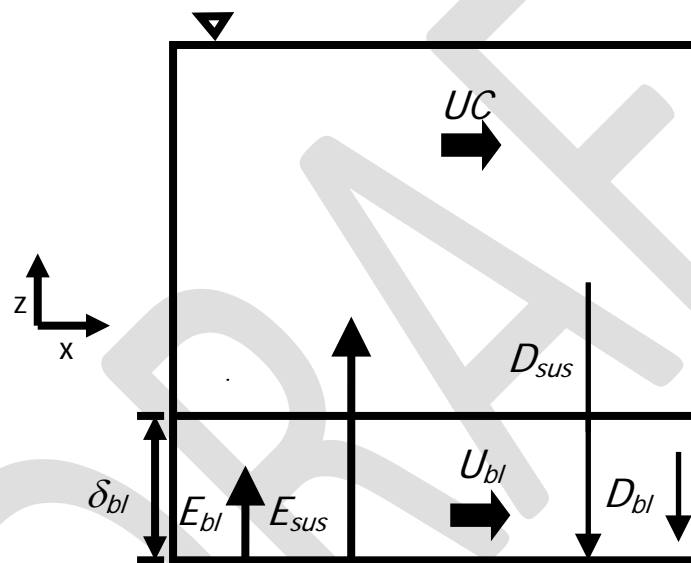


Figure B-1. Sediment transport processes simulated in SEDZLJ

- To correctly represent the processes of erosion and deposition, the sediment bed in SEDZLJ can be divided into multiple layers, some of which are used to represent the existing sediment bed and others that are used to represent new bed layers that form due to deposition during model simulations. Figure B-2 shows a schematic diagram of this multiple bed layer structure. The graph on the right hand side of this figure shows the variation in the measured gross erosion rate (in units of *cm/s*) with depth into the sediment bed as a function of the applied skin friction. A SEDFLUME study is normally used to measure these erosion rates.

- Erosion from both cohesive and non-cohesive beds is affected by bed armoring, which is a process that limits the amount of bed erosion that occurs during a high-flow event. Bed armoring occurs in a bed that contains a range of particle sizes (e.g., clay, silt, sand). During a high-flow event when erosion is occurring, finer particles (i.e., clay and silt, and fine sand) tend to be eroded at a faster rate than coarser particles (i.e., medium to coarse sand). The differences in erosion rates of the various sediment particle sizes creates a thin layer at the surface of the sediment bed, referred to as the active layer, that is depleted of finer particles and enriched with coarser particles. This depletion-enrichment process can lead to bed armoring, where the active layer is primarily composed of coarse particles that have limited mobility. The multiple bed model in SEDZLJ accounts for the exchange of sediment through and the change in composition of this active layer. The thickness of the active layer is normally calculated as a time varying function of the mean sediment particle diameter in the active layer, the critical shear stress for resuspension corresponding to the mean particle diameter, and the bed shear stress. Figure B-3 shows a schematic of the active layer at the top of the multi-bed layer model used in SEDZLJ.
- SEDZLJ can simulate overburden-induced consolidation of cohesive sediments. An algorithm that simulates the process of primary consolidation, which is caused by the expulsion of pore water from the sediment, of a fine-grained, i.e., cohesive, dominated sediment bed is included in SEDZLJ. The consolidation algorithm in SEDZLJ accounts for the following changes in two important bed parameters: 1) increase in bed bulk density with time due to the expulsion of pore water, and 2) increase in the bed shear strength (also referred to as the critical shear stress for resuspension) with time. The latter parameter is the minimum value of the bed shear stress at which measurable resuspension of cohesive sediment occurs. As such, the process of consolidation typically results in reduced erosion for a given excess bed shear stress (defined as the difference between the bed shear stress and bed shear strength) due to the increase in the bed shear strength. In addition, the increase in bulk density needs to be represented to accurately account for the mass of sediment (per unit bed area) that resuspends when the bed surface is subjected to a flow-induced excess bed shear stress. Models that represent primary consolidation range from empirical equations that approximate the increases in bed bulk density and critical shear stress for resuspension due to porewater expulsion (Sanford 2008) to finite difference models that solve the non-linear finite strain consolidation equation that governs primary consolidation in saturated porous media (Arega and Hayter 2008).

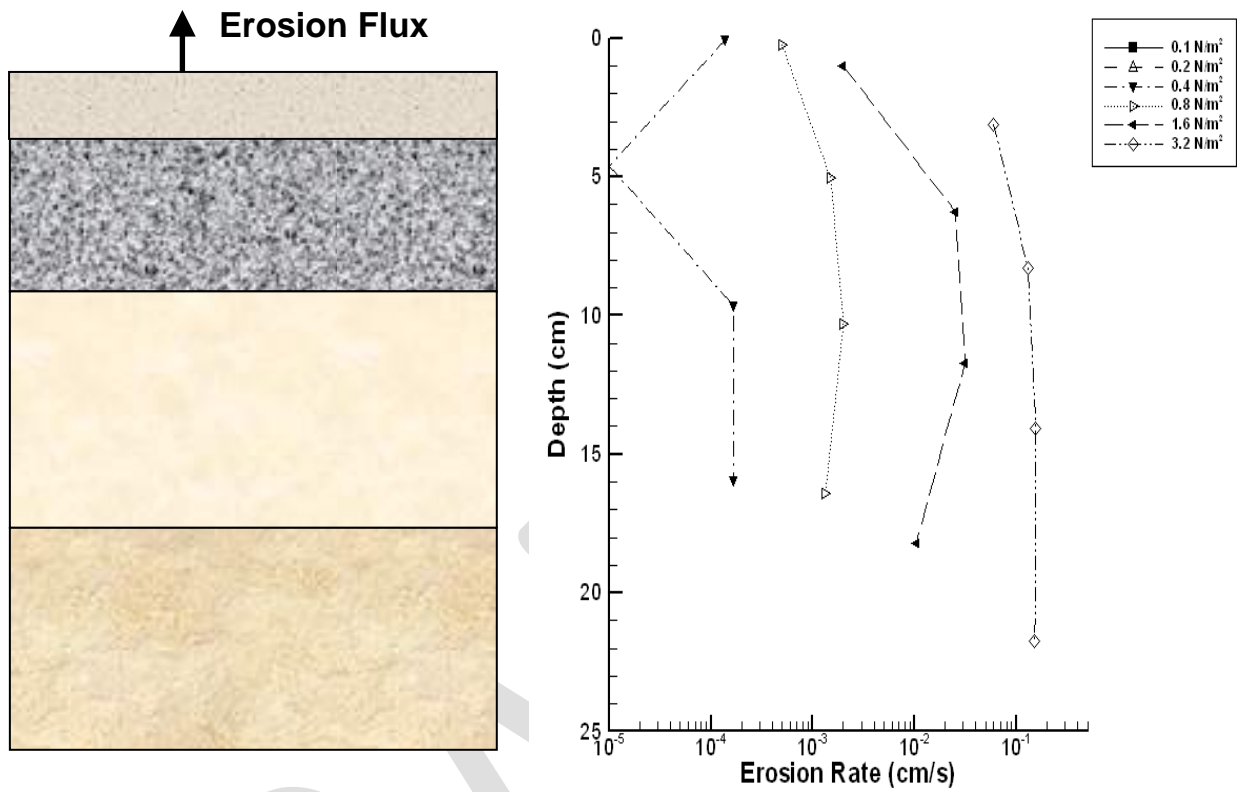


Figure B-2. Multi-Bed Layer Model used in SEDZLJ

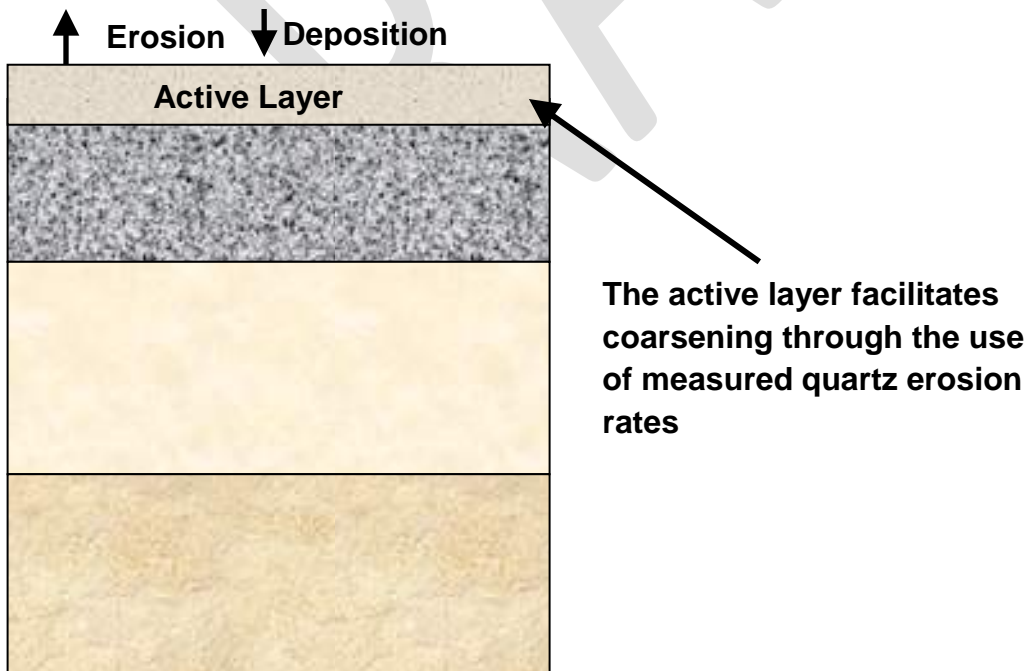


Figure B-3. Schematic of Active Layer used in SEDZLJ

An empirical-based consolidation algorithm is included in SEDZLJ. Simulation of consolidation requires performing specialized consolidation experiments to quantify the rate of consolidation. These experiments were not conducted as a component of this modeling study, and as such, consolidation was not simulated.

- SEDZLJ contains a morphologic algorithm that, when enabled by the model user, will adjust the bed elevation to account for erosion and deposition of sediment.
- SEDZLJ accounts for the effect of bed slope on erosion rates and bedload transport. The bed slopes in both the x- and y-directions are calculated, and scaling factors are applied to the bed shear stress, erosion rate, and bedload transport equations. A maximum adverse bed slope is specified that prevents bedload transport from occurring up too steep a slope.

Bedload Transport of Noncohesive Sediment

The approach used by Van Rijn (1984) to simulate bedload transport is used in SEDZLJ. The 2D mass balance equation for the concentration of sediment moving as bedload is given by:

$$\frac{\partial(\delta_{bl}C_b)}{\partial t} = \frac{\partial q_{b,x}}{\partial x} + \frac{\partial q_{b,y}}{\partial y} + Q_b \quad (\text{B-4})$$

where δ_{bl} = bedload thickness; C_b = bedload concentration; $q_{b,x}$ and $q_{b,y}$ = x- and y-components of the bedload sediment flux, respectively; and Q_b = sediment flux from the bed. Van Rijn (1984) gives the following equation for the thickness of the layer in which bedload is occurring:

$$\delta_{bl} = 0.3dd_*^{0.7}(\Delta\tau)^{0.5} \quad (\text{B-5})$$

where $\Delta\tau = \tau_b - \tau_{ce}$; τ_b = bed shear stress, and τ_{ce} = critical shear stress for erosion.

The bedload fluxes in the x- and y-directions are given by:

$$q_{b,x} = \delta_{bl} u_{b,x} C_b$$

$$q_{b,y} = \delta_{bl} u_{b,y} C_b$$

where $u_{b,x}$ and $u_{b,y}$ = x - and y -components of the bedload velocity, u_b , which van Rijn (1984) gave as

$$u_b = 1.5\tau_*^{0.6} \left[\left(\frac{\rho_s}{\rho_w} - 1 \right) gd \right]^{0.5} \quad (\text{B-6})$$

with the dimensionless parameter τ_* given as

$$\tau_* = \frac{\tau_b - \tau_{ce}}{\tau_{ce}} \quad (\text{B-7})$$

The x - and y -components of u_b are calculated as the vector projections of the CH3D Cartesian velocity components u and v .

The sediment flux from the bed due to bedload, Q_b , is equal to

$$Q_b = E_b - D_b \quad (\text{B-8})$$

where E_b is the erosion of sediment into bedload, and D_b is the deposition of sediment from bedload onto the sediment bed.